FRONTIERS OF BIOGEOGRAPHY
The scientific journal of The International Biogeography Society

Frontiers of Biogeography 18, 2025, e135871 | DOI 10.21425/fob.18.135871

RESEARCH ARTICLE

Global variability in LGM cooling amongst paleoclimate datasets affects biome reconstructions in mountains

Eline S. Rentier[1,2], Ondřej Mottl[3,4], L. Camila Pacheco-Riaño[5,6], Lotta Schultz[1,2], Julien Seguinot[7], Abe T. Wiersma[1], John-Arvid Grytnes[1,8], Suzette G. A. Flantua[1,2]

1 *Department of Biological Sciences, University of Bergen, Thormøhlens gate 53 A/B, 5006 Bergen, Norway*
2 *Bjerknes Centre for Climate Research, Bergen, Norway*
3 *Department of Botany, Charles University, Benátská 2, CZ-128 01 Prague, Czech Republic*
4 *Centre for Theoretical Study, Charles University, Jilská 1, CZ-11000, Prague, Czech Republic*
5 *Department of Biological and Environmental Sciences, University of Gothenburg, Gothenburg, Sweden*
6 *Gothenburg Global Biodiversity Centre, Medicinaregatan 7 B, 41390 Gothenburg, Sweden*
7 *Department of Water and Climate, Vrije Universiteit Brussel, Pleinlaan 2, 1050 Brussels, Belgium*
8 *Faculty of Environmental Sciences and Natural Resource Management, Norwegian University of Life Sciences, Ås, Norway*

Corresponding author: Eline S. Rentier (eline.s.rentier@gmail.com)

Editor Robert Whittaker
Received 30 August 2024 ♦ **Accepted** 30 April 2025 ♦ **Published** 29 May 2025

Abstract

Downscaled paleoclimate datasets are widely used in biogeographical research, aiding our understanding of past environmental shifts and species' responses to climate change. Numerous datasets exist, varying in spatiotemporal resolution and underlying methodologies, resulting in variation in estimated temperature. Understanding this variability is important for accurately reconstructing past biogeographical dynamics, especially in complex regions like mountains. We compare the Mean Annual Temperature (MAT) at the Last Glacial Maximum (LGM) from five different downscaled paleoclimate datasets — Beyer, CHELSA-TraCE21k, EcoClimate, PALEO-PGEM-series, WorldClim — against MAT estimates from paleoenvironmental proxy records (fossil pollen and plant macrofossils) within and outside mountains. Additionally, we test the performance of a 'global grid cooling' method (i.e. lowering local temperatures by a global LGM estimate) against proxy records. Then, we evaluate the implications of inter-dataset variability for reconstructing temperature-delimited biomes in mountains by reconstructing LGM treeline elevations. We find that LGM temperature cooling and treeline reconstructions strongly vary amongst paleoclimate datasets and between datasets and proxy records. The temperature gradient with elevation is poorly captured by datasets with a coarser spatial resolution. Paleoclimate datasets generally suggest a warmer LGM than proxy records, especially in mountains, while the global grid cooling method more closely aligns with proxy records. Inter-dataset variability can strongly affect the outcome of temperature-delimited reconstructions of biomes and their boundaries, such as treelines. We call for greater awareness and more transparency about the limitations of downscaled paleoclimate datasets in mountainous areas and suggest further research to be aimed at capturing the small-scale heterogeneity of mountains in paleotemperature datasets.

Highlights

- LGM cooling is globally both over- and underestimated by downscaled paleoclimate datasets, resulting in overestimation (i.e. too high) and underestimation (i.e. too low) of LGM treeline elevations.
- Differences in LGM treeline elevation reconstructions can range from 288 to 2779 metres, depending on the paleoclimate dataset.
- The resolution of several downscaled paleoclimate datasets is unsuitable to capture LGM temperatures in mountainous regions.
- The median temperature difference between paleoclimate datasets and proxy records is larger within than outside mountain ranges, with substantial differences amongst datasets.
- Paleoclimate dataset choice strongly impacts biogeographical hypotheses, reconstructions and conclusions and should be carefully evaluated.

Copyright *Eline S. Rentier et al.* This is an open access article distributed under the terms of the Creative Commons Attribution License (CC BY 4.0), which permits unrestricted use, distribution, and reproduction in any medium, provided the original author and source are credited.

Keywords

Biogeographical reconstructions, global grid cooling, inter-dataset variability, Last Glacial Maximum, Mean Annual Temperature, mountain regions, paleo-proxy records, paleotemperature, treeline elevation

Introduction

Paleoclimate models are essential in reconstructing past environmental conditions, providing crucial insights into the Earth's climate history. Developed over decades, these models simulate past climates by integrating atmospheric, geological and biological data that serve a wide range of scientific disciplines. Paleoclimate simulations (Box 1) enable researchers to understand long-term climate trends, assess the natural variability of the climate system and the impact of climate events on biotic and abiotic systems (e.g. Haywood et al. (2019); Kageyama and Paillard (2021)). For instance, paleoclimate simulations help biogeographers understand historical changes in species distributions (e.g. Brown et al. (2018)), allow cryosphere researchers to track glacial extents and dynamics (e.g. Ludwig et al. (2019)), aid climatologists in studying the climate sensitivity of the Earth system to atmospheric CO_2 (e.g. Annan and Hargreaves (2015); Tierney et al. (2020a)), help geoscientists model the hydrological cycle (e.g. Haywood et al. (2004)) and archaeologists to understand the effect of past climate conditions on the spatial distribution of human populations (e.g. van Andel and Davies (2003)). By simulating climate conditions during key periods, such as the Last Glacial Maximum (LGM), these models offer valuable baselines against which current and future climate changes can be assessed, making them indispensable for our understanding of the Earth's climatic past.

Since their introduction, paleoclimate models and outputs have evolved substantially and become increasingly accessible to a broad scientific community. The first climate simulations using a General Circulation Model (GCM, Box 1) were published in the late 1970s for the LGM (e.g. Gates (1976)). Proxy records such as ice cores, sediment records and fossil data aided in improving the simulations through testing and validation (e.g. Haywood et al. (2019); Tierney et al. (2020b)) and, more recently, through data-model assimilation (e.g. Tierney et al. (2020a)). Since the early 2000s, the outputs of both GCMs and Regional Circulation Models (RCM, Box 1) have been downscaled and specifically aimed to reconstruct past climate conditions. Through downscaling, the spatial and temporal resolution was enhanced to make it suitable for ecological and biogeographical applications. The availability of these high-resolution datasets facilitated widespread adoption, providing ready-to-use climatic reconstructions for the wider interdisciplinary community. Their global and spatially continuous coverage, provided in gridded

Box 1. Understanding paleoclimate: key concepts.

Here, we provide brief definitions of select terminology relevant to paleoclimate modelling, simulating and downscaling, as covered in this study.

- **Boundary conditions:** constraints that are applied to an atmospheric model to define how it interacts with its surroundings. Examples include geographical features, atmospheric chemistry and oceanic conditions and are typically fixed during the simulation. In some climate model runs, these prescribed boundary conditions are set to vary transiently over the course of the simulation. These conditions are prescribed by established experimental protocols, such as the Paleoclimate Modelling Intercomparison Project (PMIP) (Kageyama et al. 2018).
- **Downscaled paleoclimate dataset:** high-resolution climate dataset derived from (a combination of) coarser *Earth System Models* using techniques like *statistical* or *dynamical downscaling* to enhance the spatial and temporal resolution.
- **Dynamic downscaling:** a method that uses a higher-resolution regional climate model nested within a global climate model to simulate local climate conditions in greater detail and thereby produce high-resolution climate datasets (Copernicus 2021).
- **Earth System Model (ESM):** a comprehensive model of the surface Earth system, including representations of the atmosphere, ocean and land system, that runs physics-based simulations driven by *boundary conditions* of past climate dynamics, including interactions between the atmosphere, biosphere, oceans and land-surface. Most ESMs include an atmospheric *General Circulation Model*, which focuses specifically on simulating climate on a global scale (Dunne et al. 2012, 2013).
- **General Circulation Model (GCM):** a numerical model that simulates ocean and/or atmosphere circulation on a global scale. GCMs typically have a relatively coarse spatial resolution (hundreds of kilometres) due to their computational requirements (Hostetler 2015).
- **Regional Circulation Model (RCM):** uses similar physics as a GCM, but is designed for smaller areas and, thus, captures climate at a finer spatial resolution (tens of kilometres) (Hostetler 2015).
- **Simulations:** outputs of numerical models, such as ESMs, GCMs and RCMs, given the *boundary conditions* used to drive the model. Depending on the model's experimental design, simulations can be designed to reproduce real-world climate patterns or processes (although always with some bias relative to reality).
- **Statistical downscaling:** a method that uses statistical relationships between large-scale climate models and local observed climate data to produce high-resolution climate datasets (Copernicus 2021).

format (e.g. raster), were an advantage over the spatially scattered proxy records (Braconnot et al. 2012; Haywood et al. 2019). Additionally, these datasets include multiple consistent variables, opposed to the few variables that can be derived from a proxy. As a result, the datasets of downscaled paleoclimate conditions became an attractive and essential source to assess environmental conditions on regional and continental scales over deeper timescales. In this study, we focus on these datasets and refer to them as "(downscaled) paleoclimate datasets" hereafter (Box 1).

In biogeographical research, the prevalence of downscaled paleoclimate datasets has played a crucial role in enabling researchers to reconstruct historical distributions of species and ecosystems and for understanding the effect of climatic changes on current diversity patterns. Examples of such study topics include, but are not limited to, range shifts (e.g. Martínez-Meyer and Peterson (2006)), migration pathways (e.g. Garzón et al. (2008)), niche stability (e.g. Worth et al. (2014); Kandziora et al. (2024)), refugia (e.g. Svenning et al. (2011); Gavin et al. (2014)), speciation and extinction patterns (e.g. Stigall (2013)) and vegetation or biome reconstructions (e.g. Werneck et al. (2011); Collevatti et al. (2013)). Amongst the most popular datasets are WorldClim (Hijmans et al. 2005) and CHELSA-TraCE21k (Karger et al. 2023), which provide high-resolution (0.04° and 0.008°, respectively) climate data for the period since the LGM. These datasets have been instrumental in numerous studies due to their open accessibility, comprehensive climate variables ("bioclimatic variables"), global and temporal coverage and easy integration with ecological models such as Species Distribution Models (SDMs) and Ecological Niche Models (ENMs) (Varela et al. 2015).

The LGM has been a period of especially high interest for climatic and ecological reconstructions. It represents a time of significant climatic contrast, providing a benchmark for understanding the impacts of extreme climate conditions on ecosystem and species distributions (Varela et al. 2015; Carotenuto et al. 2016). LGM estimates have been frequently used to study, quantify and test, for example, refugia (e.g. Tang et al. (2018)), phylogenetic hypotheses (e.g. Muellner-Riehl et al. (2019)) and species and biome distributions (e.g. Svenning et al. (2011); Kandziora et al. (2024)), often aided by SDMs and ENMs (e.g. Nogués-Bravo (2009); Varela et al. (2011)). Additionally, these estimates are used for studies based on climate derivatives over time, such as climatic stability (e.g. Harrison and Noss (2017); Brown et al. (2020)) and climate change velocity (e.g. Sandel et al. (2011)). Evidently, paleoclimatic data are essential to support numerous applications, from testing ecological and evolutionary hypotheses to understanding species and biome responses to extreme and dynamic climate conditions.

Though paleoclimate datasets all provide global coverage and paleotemperature estimations, they vary vastly in spatial resolution, temporal resolution, and temporal range (Barreto et al. 2023). Moreover, they are based on different GCMs that each have their parameterisations and can, therefore, differ substantially (Varela et al. 2015). Inter-dataset variation can impact findings derived from biogeographical studies (Collevatti et al. 2013), but underlying methodologies and uncertainties are often difficult to grasp for those outside the climatology community (Lima-Ribeiro et al. 2015; Varela et al. 2015). In addition, previous paleoclimatic studies have shown that, while simulations can generally capture the direction of climatic changes from the LGM to the pre-industrial period, they perform poorly in estimating the magnitude of change. In comparison to proxy records, simulations tend to overestimate LGM sea surface cooling in the Tropics (Waelbroeck et al. 2009) and underestimate LGM land cooling (Masson-Delmotte et al. 2005; Kageyama et al. 2006; Bartlein et al. 2011; Braconnot et al. 2012). Harrison et al. (2013) quantified these discrepancies for a range of different simulations, showing that all simulations derived from CMIP5 and PMIP2 consistently underestimate LGM temperatures over land. Mountain regions might be especially prone to potential discrepancies due to larger temperature changes at high elevation during the LGM (Harrison 2005; Loomis et al. 2017), but this has not been tested so far.

Paleoclimate simulation and downscaling in mountain regions present specific challenges (Badgley et al. 2018). Mountains exhibit stark differences in both biotic and abiotic factors over small spatial scales (Shafer et al. 2005). Complex environments and topography create elevational gradients, microclimates and diverse habitats within a close geographical range that are challenging to capture accurately in simulations (Lima-Ribeiro et al. 2015). The more complex the topography, the more temperature information is lost with decreasing spatial resolution of the climate simulation. In addition, mountain regions often have sparse weather stations and limited historical climate data (Hik and Williamson 2019; Pepin et al. 2022), hindering accurate calibration and validation of downscaled climate data in mountains and resulting in less reliable predictions (Thornton et al. 2022). Given the wide usage of paleoclimate datasets by the biogeographical community, it is essential to assess their applicability in mountains from the perspective of biogeographical reconstructions.

In this study, we assess paleoclimate data variability in mountains by comparing estimated Mean Annual Temperature (MAT) at the LGM derived from five different downscaled paleoclimate datasets — Beyer, CHELSA-TraCE21k, EcoClimate, PALEO-PGEM-series, WorldClim — (Table 1) against a validation compilation of paleoenvironmental proxy records. Our objective is to investigate how these temperature estimations differ worldwide and test if substantial difference exists between paleoclimate datasets and within and outside mountain ranges. We further compare outcomes with a so-called 'global grid cooling' method where we lower the world's temperature by a global LGM estimate. To showcase the impact of inter-dataset variability and its potential implications for biogeographical research, we reconstruct treelines at the LGM using the MAT estimations of the paleoclimate datasets. Treelines, which typically occur at high elevation in mountain ranges, but also include the polar treeline, delineate different biomes and serve as important ecological boundaries

Table 1. Overview of downscaled paleoclimate datasets used in this research. Datasets are ordered from highest to lowest spatial resolution.

Downscaled paleoclimate dataset	Spatial resolution (°)	Temporal resolution (yr)	Temporal range (BP)	Reference
CHELSA-TraCE21k	0.008	100	21 kyr	(Karger et al. 2023)
WorldClim 1	0.04	Snapshot	Snapshot at 6 ka, 22 ka, 120 ka	(Hijmans et al. 2005)
Beyer et al.	0.5	1–2 k	120 kyr	(Beyer et al. 2020),
EcoClimate	0.5	Snapshot	Snapshot at 6 ka, 21 ka, 3.3–3.0 Ma	(Lima-Ribeiro et al. 2015)
PALEO-PGEM-Series	1	1 k	5 Myr	(Barreto et al. 2023)

and transition zones (Jobbágy and Jackson 2000; Körner 2007; Cairns 2013; Greenwood and Jump 2014). This makes treelines an excellent subject for comparing paleoclimate datasets because they are climate-delimited with a particular sensitivity to temperature (Paulsen and Körner 2014; Körner 2021), thus relying heavily on accurate temperature estimations. By focusing on the treeline in mountains globally, we aim to provide insights into the variations and consistency of paleoclimate datasets in mountainous areas, informing future biogeographic and ecological research.

Background

The Last Glacial Maximum as a benchmark period

The LGM of the last glacial cycle is commonly defined as the time of global maximum land ice volume (Clark et al. 2009). For the 'global' LGM, different time intervals are found in literature (see review in Hughes et al. (2013)), but the LGM is most commonly stated to have been around 21 ka BP (thousand years before present). The LGM's prominence as a target period in paleoclimate research is due to its distinct climatic conditions (greenhouse gas concentration, atmospheric CO_2; Cao et al. (2019)), extensive ice sheets (Mix et al. 2001), high coverage of well-dated proxy temperatures (Zhu and Poulsen 2021) and profound impacts on global ecosystems (Nolan et al. 2018). The period's climatic contrast to the present day, combined with abundant, well-preserved proxy data, has facilitated simulation, validation and calibration of a suite of climate models (see reviews by Bartlein et al. (2011); Harrison et al. (2016)). The LGM has served as a useful test case for assessing paleoclimate models, aiding in the evaluation and improvement of their accuracy. Comparing the LGM with other periods of climatic extremes, such as interglacial epochs or earlier glacial maxima, has expanded research into the Earth's climate system's range and variability over geological timescales (Jansen et al. 2007). These paleoclimatic simulation-proxy comparisons have been used to validate simulations and test state-of-the-art Earth System Models (ESM, Box 1), as well as studying the sensitivity of the Earth system to variations in atmospheric CO_2 (Tierney et al. 2020a), enhancing confidence in their projections for future climate conditions (Harrison et al. 2016).

Proxy records

In paleoclimate research, there are two primary ways to estimate past climates: using simulations from paleoclimate models and using reconstructions derived from proxy records. The latter come from various natural archives, including marine sediments, terrestrial deposits and ice cores (Waelbroeck et al. 2009; Harrison et al. 2016). Terrestrial proxy records, such as fossil pollen records, stable isotopes and organic biomarkers, offer insights into past vegetation, temperature and precipitation. These records, also called paleo(environmental) proxies or 'environmental sensors', are typically analysed statistically to reconstruct past climate conditions (Kohfeld and Harrison 2000; Bartlein et al. 2011; Braconnot et al. 2012), which can then be used to make quantitative comparisons with paleoclimate simulations (Braconnot et al. 2012). Over the years, several different continental and global compilations (syntheses) of proxy records that cover the LGM have been built (see supplementary materials of Braconnot et al. (2012)). More recently, proxy-based reconstructions have been combined with multiple paleoclimate simulations to achieve an integrated statistical inference. This process is called 'paleoclimate data assimilation' and has promising potential to develop an estimate of the state of the climate at a particular place and moment in time (see, for example, Tierney et al. (2020a) and Osman et al. (2021)). However, a full view of the LGM climate state is still much in process as proxies are unevenly distributed, their uncertainties still need to be tackled and methods for such inference are under development (Tierney et al. 2020a; Erb et al. 2022).

Methods

Workflow

This study is divided into two parts (Fig. 1). The first part constitutes of comparing LGM temperature estimations of downscaled paleoclimate datasets (Fig. 1A) including a homogeneous global cooling method (Fig. 1C) against compilations of proxy records (Fig. 1B). The global cooling method is hereafter referred to as global grid cooling (GGC/ggc in figures and variable names). The second phase consists of a pre-processing step: calculating the LGM temperatures of the global grid cooling (Fig. 1D) and then comparing LGM treeline reconstructions, based on

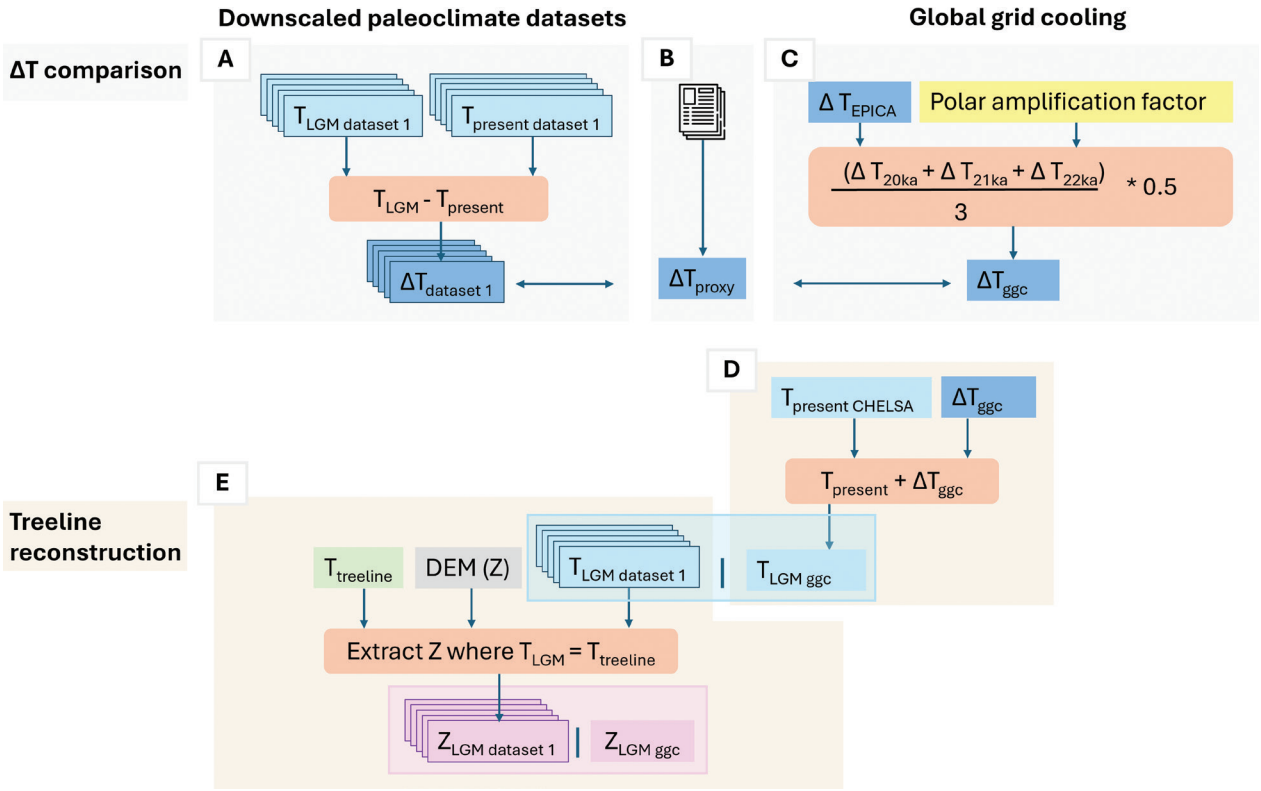

Figure 1. Workflow for the delta Temperature (ΔT) comparison and treeline reconstruction for downscaled paleoclimate datasets and global grid cooling. **A.** For all five paleoclimate datasets — Beyer, CHELSA-TraCE21k, EcoClimate, PALEO-PGEM-series, WorldClim — the ΔT is calculated by subtracting the present-day temperature raster from the LGM temperature raster; **B.** ΔT_{proxy} values are derived from a compilation of proxy records (fossil pollen and plant macrofossil) obtained from Farrera et al. (1999); Bartlein et al. (2011); **C.** For the global grid cooling, the ΔT is calculated by averaging ΔT values over three thousand years from the EPICA ice core (20–22 ka BP) and multiplying this by the polar amplification factor (0.5); **D.** A pre-processing step is taken to calculate the $T_{LGM\text{-}ggc}$ from the present-day CHELSA-TraCE21k temperature raster and the earlier calculated ΔT_{ggc}; **E.** Treeline elevation (Z) is extracted where $T_{LGM} = T_{Treeline} \pm 0.25$ degrees. This is repeated with the LGM temperatures of all the datasets ($T_{LGM\ dataset(n)}$) and the global grid cooling ($T_{LGM\text{-}ggc}$). T: Temperature, LGM: Last Glacial Maximum, Z: Elevation, DEM: Digital Elevation Model, ka: thousand years BP.

the different downscaled paleoclimate datasets (Fig. 1E). The comparison of both parts is done on a global scale, using the Global Mountain Biodiversity Assessment (GMBA) standardised mountain inventory (V2, level 3) to delineate mountain ranges (Snethlage et al. 2022). These spatial analyses were done in ArcGIS Pro (version 3.1.0) and Python (version 3.11). All visualisations and regression models were made using R (version 3.6.2). An overview of all datasets used can be found in Table 2 and all code and data required to perform the analysis and visualisations are available as a GitHub release on Zenodo: https://doi.org/10.5281/zenodo.14228272.

Temperature change (present-LGM) reconstruction based on paleoclimate datasets

We included five downscaled paleoclimate datasets (Table 1) with varying spatiotemporal resolution and based on various climate models and downscaling approaches (see Table 2). For each dataset, we calculated the MAT change ($\Delta T = T_{LGM} - T_{present}$) between the present (~ 1950 CE) and LGM (~ 21ka BP) rather than the absolute LGM temperature to allow for a direct comparison to proxy records. MAT, also known as bioclimatic factor 1 (bio1), is hereafter referred to only as "temperature". Though more downscaled paleoclimate datasets are freely available (e.g. PaleoClim (Brown et al. 2018), Krapp et al. (Krapp et al. 2021), WorldClim 2 (Fick and Hijmans 2017) and Oscillayers (Gamisch 2019)), we only selected datasets with temperatures for both the LGM and the present. When needed, the temperature rasters (i.e. grid of pixels) were transformed from their original format (see Table 2) to a GeoTIFF format, and the projection was standardised to WGS84 for all rasters.

Temperature change (present-LGM) reconstruction based on global grid cooling

A simplified method of estimating the temperature at the LGM was achieved by calculating the global mean temperature change between the present and LGM (Fig. 1C) and then subtracting this change from every cell in a temperature raster (Fig. 1D). The calculated temperature change was used in our comparison analysis with proxy

Table 2. Overview of used datasets, their year of publication, source and (if applicable) filename.

Name	Year	Source (publication)/(dataset, filename)
EPICA Dome C Ice Core	2007	(Jouzel et al. 2007)/(Jouzel and Masson-Delmotte 2007)
GMBA mountain inventory V2.0	2018	(Snethlage et al. 2022)/(Snethlage et al. 2021)
GMTED global elevation data	2010	(Danielson and Gesch 2011)
Downscaled paleoclimate datasets		
CHELSA-TraCE21k	2023	(Karger et al. 2023) **Present**: CHELSA_TraCE21K_bio01_20_V1.0.tif
		LGM: CHELSA_TraCE21K_bio01_-190_V1.0.tif
Beyer et al.	2020	(Beyer et al. 2020) **Present:** Late_Quaternary_Environment_-20.nc
		LGM: Late_Quaternary_Environment_-21020.nc
EcoClimate	2015	(Lima-Ribeiro et al. 2015)
		Present: bio#CCSM_Modern(1950–1999)_bio1.bil
		LGM: bio#baseline_Modern(1950–1999)#CCSM_LGM (21ka)_bio1.bil
PALEO-PGEM-Series	2023	(Barreto et al. 2023)/(Baretto et al. 2022)
		Present: PALEO-PGEM-Series_bio1_mean_-20.nc
		LGM: PALEO-PGEM-Series_bio1_mean_-21020 (21ka).nc
WorldClim 1	2005	(Hijmans et al. 2005) **Present**: ccmidbi_6ka_2.5.tif
		LGM: cclgmbi_21ka_2.5.tif
Compilation of proxy records		
Farrera et al.	1999	(Farrera et al. 1999)
Bartlein et al.	2011	(Bartlein et al. 2011)

data and LGM treeline reconstruction. Such grid-based cooling has been used, for example, by Chala et al. (2017) for the alpine biome in tropical Africa using a regionally derived LGM temperature estimate from a pollen record. This method allowed us to adjust for the global temperature change on a per-pixel level and, thus, keep the spatial resolution of the present-day temperature raster.

In our analysis and for simplification, we derived the average Antarctic temperature change from the EPICA dome ice core record (Jouzel et al. 2007). The global mean surface temperature change was then calculated by averaging the Antarctic temperature values from EPICA between 20–22 ka BP and multiplying it by the standard polar amplification factor: 0.5 (Hansen et al. 2013) (Suppl. material 1: table S1). The resulting ΔT_{ggc} was -4.673 °C, which falls within the range of simulation results (e.g. 3–7 °C (Masson-Delmotte et al. 2005), 2.2–5.5 °C (Tierney et al. 2020a), 4.5 ± 0.9 °C (Annan et al. 2022)). We acknowledge that research continues to debate global mean cooling estimates and the wide estimates ranges due to proxy and simulation uncertainties (Schneider von Deimling et al. 2006; Tierney et al. 2020a; Osman et al. 2021). We opted for a grid-based cooling for comparison purposes and to showcase the approach of estimating large-scale regional temperature change inferred from a proxy record to constrain regional LGM climate (Schneider von Deimling et al. 2006).

Temperature change reconstruction vs proxy records

The calculated ΔT rasters from the paleoclimate datasets and the ΔT_{ggc} were compared to proxy data (Fig. 1A, B, C). We used two high-quality compilations of proxy datasets (Farrera et al. 1999; Bartlein et al. 2011) totalling up to n = 174 records to ensure good global coverage within (n = 59) and outside (n = 115) mountain ranges (Fig. 2). The proxies from both datasets come from fossil pollen and plant macrofossil data derived from ^{14}C-dated sediment records. The proxy compilations contain the ΔT values for numerous locations, representing the estimated temperature change between the present and LGM. The proxy dataset from Bartlein et al. (2011) contained ready-to-use ΔT values, whereas the ΔT values from Farrera et al. (1999) were extracted from their tables and cleaned before use. The cleaning process consisted of removing all proxies without ΔT values and those only stating "warmer" or "cooler" for the temperature change. When proxies contained a range for the ΔT values, rather than an exact number, the mean was taken. At the location of each proxy, we extracted the ΔT value from the rasters of the paleoclimate datasets and global grid cooling method. Next, we calculated the temperature difference ($\Delta T_{difference} = \Delta T_{dataset} - \Delta T_{proxy}$) to compare temperature estimates from the paleoclimate datasets and the global grid cooling to the proxy records (Fig. 1A, B, C). We performed a linear regression analysis to test whether being "within" a mountain range or not (i.e. "outside") had a significant effect on the temperature difference. Furthermore, we illustrated the relationship between latitude and the temperature difference by fitting a hierarchical Generalised Additive Model (HGAM), as we could not assume a linear relationship. For the HGAM, we used Restricted Maximum Likelihood (REML) with $\Delta T_{difference}$ as a response variable and latitude as group-level smoothers (predictor) (i.e. model S by Pedersen et al. (2019)) for both within and outside mountain ranges, with the formula: $\Delta T_{difference} \sim$ s(latitude, within_outside_factor, bs = "fs", k = 5, m = 2).

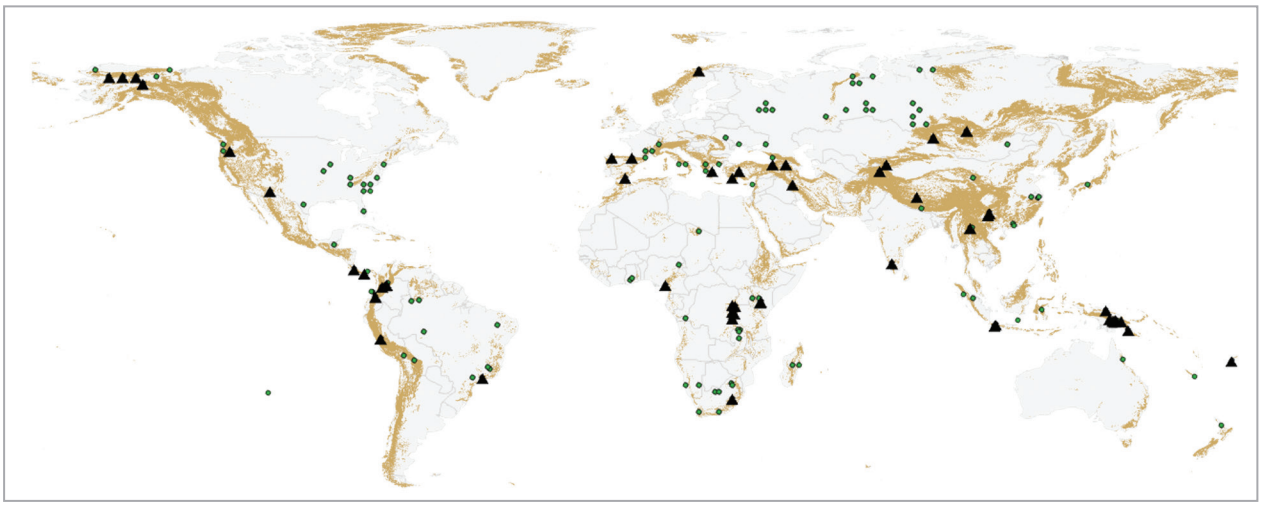

Figure 2. Distribution of proxy records that fall within (triangles, n = 59) and outside (points, n = 115) the GMBA mountain ranges (brown). Data references: Farrera et al. (1999); Bartlein et al. (2011). GMBA mountain ranges by Snethlage et al. (2022). Basemap powered by Esri et al. (2015).

Reconstruction of treeline elevations at the LGM

Treeline definition

Treelines occur at different elevations (Testolin et al. 2020) and temperatures (Körner and Paulsen 2004) across the globe. A commonly used generalised treeline delimitation is that of Körner and Paulsen (2004) and is based on a seasonal mean ground temperature of 6.7 °C ± 0.8 °C SD, with slightly higher values in temperate regions (7–8 °C) and slightly lower in equatorial regions (5–6 °C). Although varying other factors have been attributed to influencing treeline position (e.g. mass elevation effect (Kienle et al. 2023), geomorphology (Körner 2021; Kienle et al. 2023), continentality (Kienle et al. 2023), precipitation levels and drought (Daniels and Veblen 2004), anthropogenic influences (Körner and Paulsen 2004)), temperature is the primary driver (Körner and Paulsen 2004).

A treeline that follows a common isotherm, often at high elevations or high latitudes, is called a climate- or temperature-delimited treeline. A temperature-delimited treeline represents the potential treeline, without considering taxon-, land use- or fire-driven limits and is, therefore, well-suited for paleoreconstructions. In reality, however, treelines often deviate from their thermal limit due to non-climatic drivers (Körner and Hoch 2023) and are then called realised treelines and are better suited for present-day analysis (e.g. Testolin et al. (2020)). We opted for a temperature-delimited treeline, based on Beck et al. (2023) following the approach proposed by Kandziora et al. (2024). We determined the temperature-delimited treeline, hereafter "$T_{Treeline}$", by extracting the temperature based on CHELSA V.2.1 (Karger et al. 2017), at which the present-day treeline is located for each GMBA mountain range with alpine biome (class 29, ET; Polar, tundra, see Beck et al. (2023)).

LGM treeline reconstruction

In preparation of the treeline reconstruction, we first calculated the LGM temperatures for the global grid cooling method. We derived the present-day temperature raster from CHELSA-TraCE21k (Karger et al. 2023) and subtracted the earlier calculated ΔT_{ggc} value from each individual pixel to obtain the $T_{LGM\text{-}ggc}$ raster (Fig. 1D). Then, we used the T_{LGM} rasters of each paleoclimate dataset and the $T_{LGM\text{-}ggc}$, together with the temperature at which the treeline occurs ($T_{Treeline}$) to extract the elevation (Z) at which the $T_{treeline}$ equalled the T_{LGM} (Fig. 1E). We used a margin of 0.25 °C of the $T_{Treeline}$ to account for resolution constraints. This approach ensures that pixels approximately representing the target temperature value are included, despite slight deviations caused by a coarse resolution. The Global Digital Elevation Model by Danielson and Gesch (2011) was resampled to match the spatial resolution of each paleoclimate raster (Table 2). By resampling the elevation model rather than the paleoclimate rasters, we ensured that the observed differences accurately reflect the values as given by the dataset, allowing a fair comparison of the data. To allow a comparison of the reconstructed treelines derived from both methods, we computed zonal statistics (ArcGIS Pro) for each mountain range to obtain the minimum, maximum, mean and standard deviation of the treeline elevations within each mountain range.

Results

Spatial resolution of paleoclimate datasets

Paleoclimate datasets exhibit substantial variability in spatial resolution (Table 1, Fig. 3A, C). To show the effect of resolution, we compared the temperature gradient with elevation and focused on the Central European Highlands as a case study. While we anticipated a linear relationship due to the

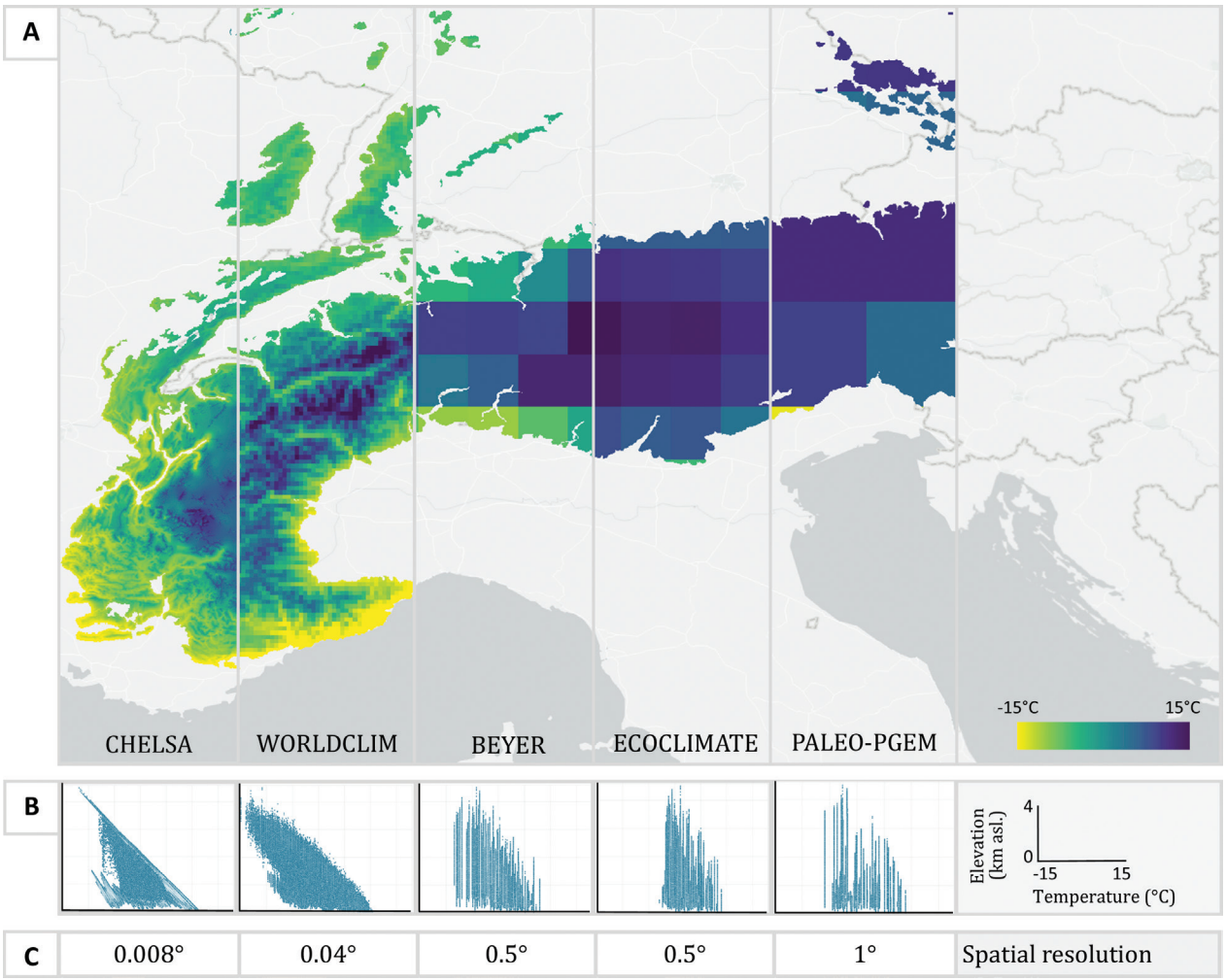

Figure 3. Comparison of spatial resolution and elevational changes of temperature of downscaled paleoclimate datasets for the Central European Highlands. **A.** Mean annual temperature of each paleoclimate dataset; **B.** Mean Annual Temperature distribution (x-axis) along elevation (y-axis, km above sea level) for each dataset for the entire mountain range. Temperature values are displayed as blue dots. Vertical lines are formed when a single temperature value (on the x-axis) corresponds to a wide range of elevations (on the y-axis); **C.** Spatial resolution of each dataset. See Table 1 for data references. Basemap powered by Esri et al. (2015).

lapse rate, coarse resolution datasets failed to capture the finer-scale temperature variations associated with elevation. This is evident in the barcode-like scatterplots of Beyer, EcoClimate and PALEO-PGEM, where a single temperature value (x-axis) corresponds to a wide range of elevations (y-axis), forming vertical lines (Fig. 3B). In contrast, high-resolution datasets like CHELSA-TraCE21k and WorldClim display a more natural trend, as temperature decreases more consistently as elevation increases. Thus, the varying spatial resolutions considerably affect the capturing of climatic information, highlighting the critical importance of considering the resolution when using paleoclimate data in mountains.

LGM cooling estimates

In general, we observe that paleoclimate datasets tend to estimate higher (i.e. warmer) temperature values for the LGM than proxy records (Fig. 4) with this discrepancy being more pronounced within mountain ranges. Outside mountains, the median $\Delta T_{difference}$ of WorldClim, Beyer and EcoClimate are closest to proxy estimates (deviating with -0.08 °C, 0.28 °C and 0.14 °C, respectively), while CHELSA-TraCE21k, PALEO-PGEM and global grid cooling show less LGM cooling than indicated by proxy records (deviating with 1.11 °C, 1.35 °C and 1.33 °C, respectively). Within mountains, all datasets estimate higher LGM temperatures than proxy records, with global grid cooling showing the highest agreement (median $\Delta T_{difference}$ of 0.33 °C (global grid cooling) vs. 2.1 °C (CHELSA-TraCE21k), 0.8 °C (WorldClim), 1.27 °C (Beyer), 0.9 °C (EcoClimate) and 1.38 °C (PALEO-PGEM)). However, the effect of being either within or outside a mountain range was not significant, except for the global grid cooling method (see Suppl. material 1: table S2 for an overview of all p-values). For the global grid cooling method, the differences with the proxy records are significantly ($p < 0.01$) smaller within mountain ranges than outside. PALEO-PGEM exhibits almost no difference in median $\Delta T_{difference}$ (deviating with 1.35 °C "outside" vs. 1.38 °C "within"), likely due to its low spatial resolution. We also observe several outliers with

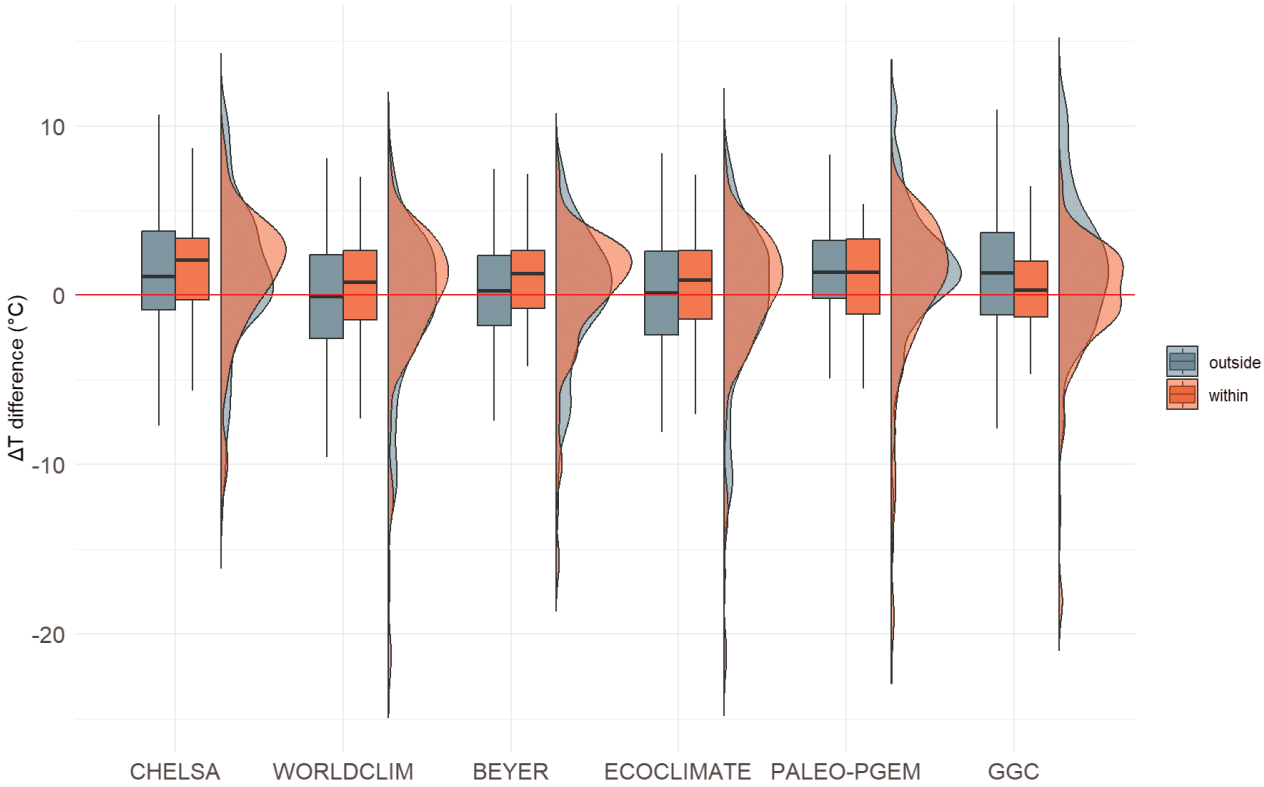

Figure 4. Differences in LGM cooling (ΔT) estimates and distribution between downscaled paleoclimate datasets and proxy records within (orange, n = 59) and outside (grey, n = 115) mountain ranges. The red line at $\Delta T_{difference}$ = 0 indicates where the dataset and proxy are equal. GGC = global grid cooling. The boxplots show 50% of the data inside the box; the bottom edge representing the 25th percentile, the middle line the median and the bottom edge the 75th percentile. The whiskers extend to the smallest and largest values of the dataset within 1.5* the interquartile range between the 25th and 75th percentile. The half-violin plots display a smoothed distribution of the values as displayed in the boxplots, but where the width indicates the density of data and the long whiskers display the full data range.

a large negative $\Delta T_{difference}$ value, indicating that paleoclimate datasets estimated much lower temperatures (i.e. overestimated LGM cooling) than proxy records indicate for those locations. Intra-dataset variability is evident both within and outside mountain ranges, shown by the long whiskers of the box plots (Fig. 4). These findings highlight the differences in LGM estimates amongst datasets and between datasets and proxies, as well as highlight the challenges in reconstructing past climates in mountains.

LGM temperature estimates also vary substantially across the globe, yet the direction of dataset-proxy disagreement often concurs amongst datasets (Fig. 5). We found consistent trends of underestimating LGM cooling by downscaled paleoclimate datasets across the tropical mountains of Central and South America, such as the northern and central Andes and South Africa. While datasets tend to estimate higher LGM temperatures (i.e. underestimated cooling) in the east coast of North America, estimates are often much lower than proxy records (i.e. overestimated cooling) in the west and northwest of the continent, as is also the case for continental Asia, Southeast Asia and Oceania. Contrasting patterns within continents are likewise observed across Africa, such as between the East African Rift and South Africa.

When assessing the relationship with latitude, the observed trends of dataset-proxy temperature differences are relatively stable within mountains across datasets for the Southern Hemisphere, but vary in the Northern Hemisphere. Outside mountains, we observe more flexibility in the curve, especially in the temperature regions in the Northern Hemisphere. We see that paleoclimate datasets slightly underestimate LGM cooling in the Southern Hemisphere, while LGM cooling is overestimated towards the Northern Hemisphere (Fig. 6), both within and outside mountains. One exception to this trend is the $\Delta T_{difference}$ values of the global grid cooling method outside mountain ranges. Here, the data underestimate LGM temperatures towards the Northern Hemisphere. We also observe that the outliers with a large negative $\Delta T_{difference}$ values are located primarily in the Northern(most) Hemisphere. These findings emphasise the prominent spatial variability of LGM temperature estimates, with deviations influenced by latitude, particularly in mountainous regions.

Comparison of reconstructed LGM treeline elevations

Elevational differences amongst reconstructed LGM treelines from downscaled paleoclimate datasets exist globally and can range from 288 m in the Cameroon line in the Central African Highlands to 4779 m in the southern

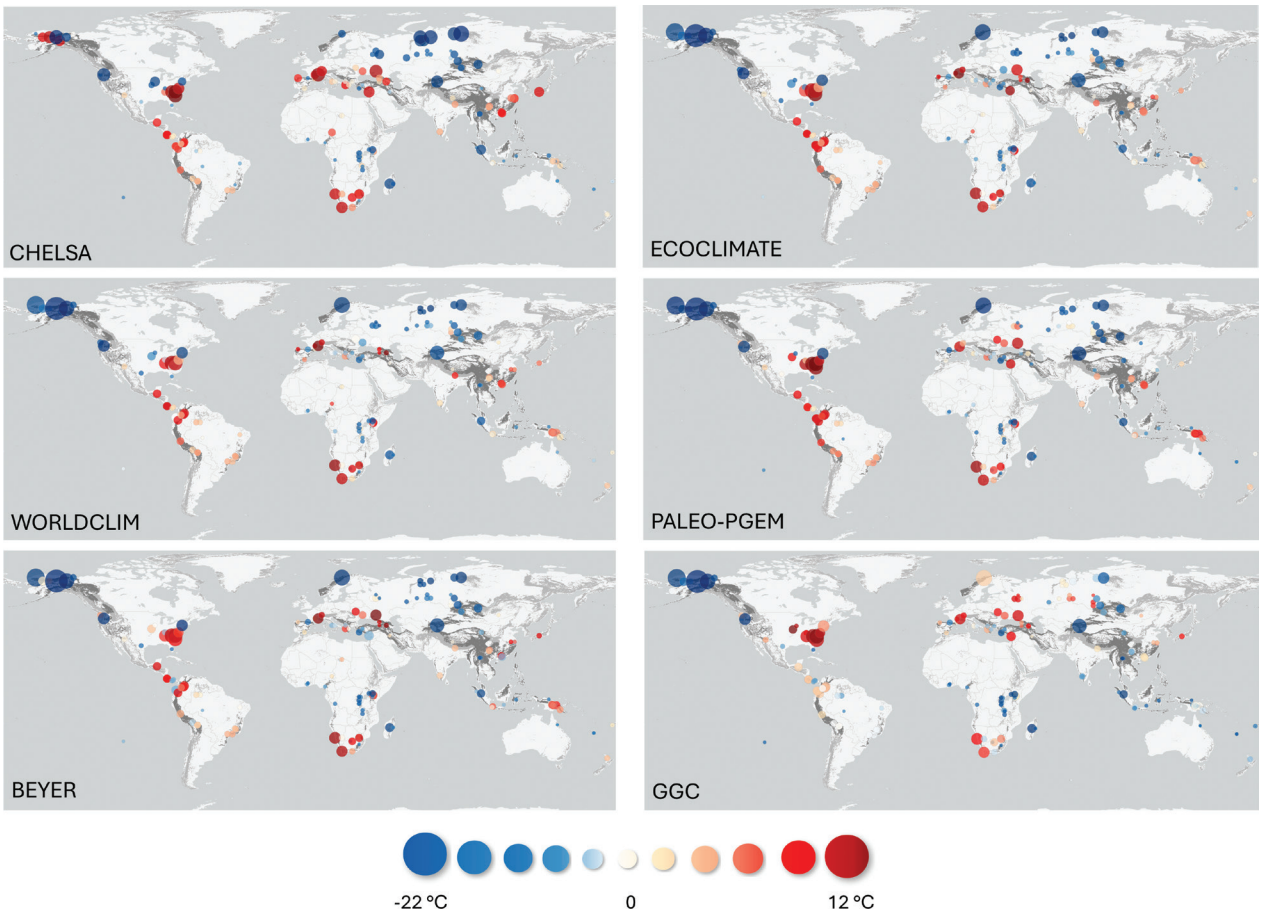

Figure 5. Differences in LGM cooling (ΔT) estimates between downscaled paleoclimate datasets and proxy records. Positive values (red) indicate that the dataset estimated a warmer LGM (i.e. higher temperature) than the proxy record, while negative values (blue) indicate a cooler LGM (i.e. lower temperature). The bubble size represents the magnitude of the difference between the proxy record (baseline) and the LGM temperature estimations by the datasets. Zeros indicate no difference between the proxy and dataset. Mountain ranges (GMBA, Snethlage et al. (2022)) are coloured dark grey if they contain proxy data and light grey if not. GGC = global grid cooling. See Table 1 for data references. Basemap powered by Esri (Esri et al. 2015).

Andes (Fig. 7A, B). Mountain ranges where LGM treeline elevations differ more than 3000 m are found especially across the Americas (e.g. Rocky Mountains, Pacific Coast Ranges, Cordillera de la Costa and the southern Andes). General trends of reconstructed LGM treeline elevations follow a similar latitudinal pattern as present-day treeline elevation. We observe lower treelines towards the north (e.g. Arctic Cordillera, the Anadyr Highlands and the Chukotka Mountains), higher treeline elevations around the Equator (e.g. Pamir Mountains, Himalaya and central Andes) and lower treelines again towards the south of the Southern Hemisphere (e.g. Tasmania, South Island (New Zealand) and the Falkland Islands) (Fig. 7B).

Within mountain ranges, reconstructed treeline elevations vary vastly depending on which dataset is used. Disagreements amongst datasets are observed inconsistently across mountain ranges. Some vary strongly (e.g. Tian Shan, Hindu Kush and central Andes), whereas others show better agreement (e.g. East European Highlands, Balochistan Ranges and Tasmania). The length of the whiskers (i.e. vertical lines; Fig. 7B) for each dataset indicates the estimated range of treeline elevations within the same mountain range. We see that these are generally longer for higher resolution datasets (e.g. CHELSA-TraCE21k) and shorter for lower resolution datasets (e.g. PALEO-PGEM), likely related to differences in resolution. For some datasets, we could not reconstruct the LGM treeline as these datasets lack corresponding LGM temperatures (Fig. 7C). This is the case especially for smaller mountains ranges and islands (e.g. Iceland, The Prince Edward Islands and the Falkland Islands). Most mountain ranges are captured by the global grid cooling method (70 out of 75) and CHELSA-TraCE21k (67 out of 75). Thus, dataset choice is crucial for mountains and specifically LGM treeline reconstructions.

Discussion

Our analysis reveals several key findings about LGM temperature estimations from downscaled paleoclimate datasets and their impact on treeline reconstructions. Firstly, paleoclimate datasets exhibit substantial variability in spatial resolution, indicating that the precision of these datasets can vary considerably, particularly in mountain ranges. Secondly,

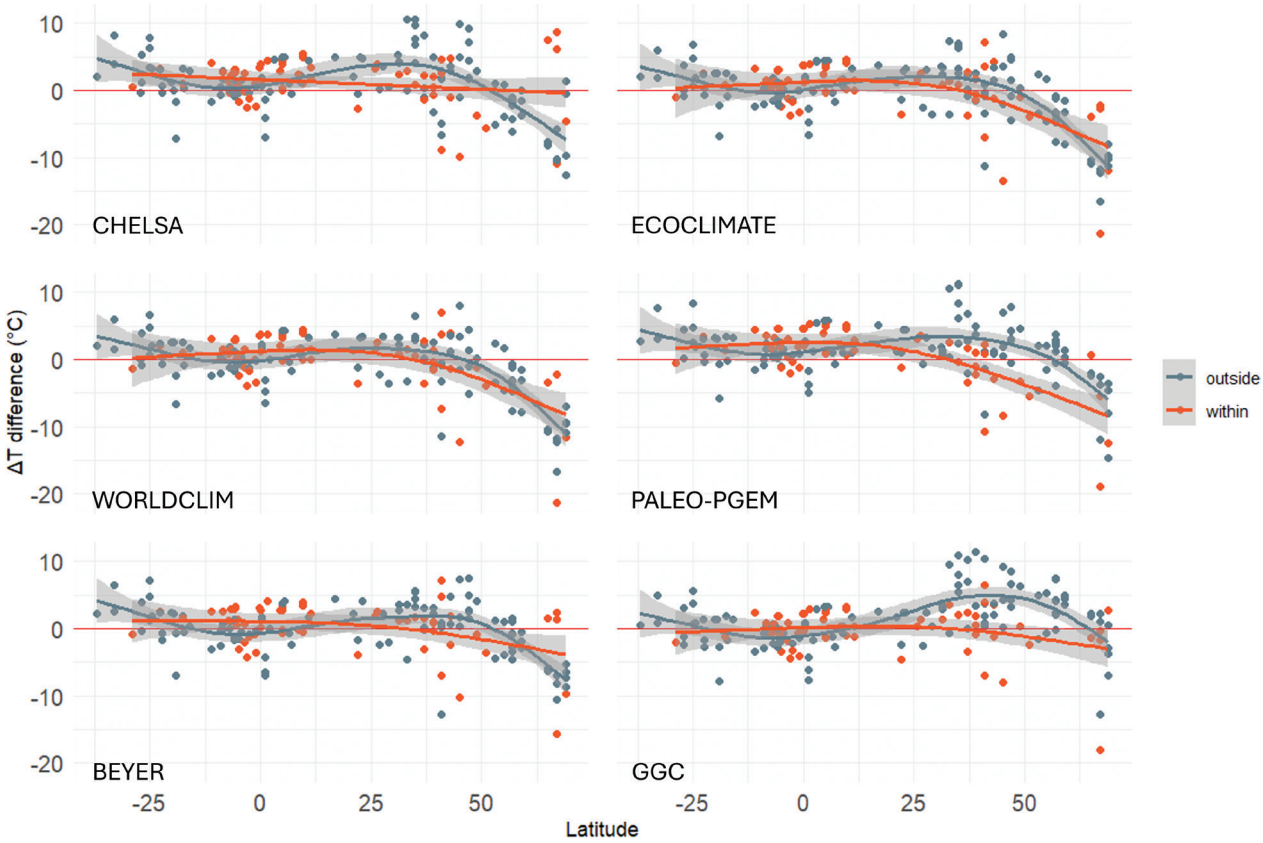

Figure 6. Differences in LGM cooling (ΔT) estimates between downscaled paleoclimate datasets and proxy records along a latitudinal gradient. The horizontal red line at $\Delta T_{difference}$ = 0 indicates where the estimated temperature by the dataset and proxy is equal. The points represent proxy locations within (orange) and outside (grey) mountain ranges. The hierarchical Generalised Additive Model (HGAM) lines have a 95% confidence interval. GGC = global grid cooling. See Table 1 for data references.

we observe that paleoclimate datasets tend to generally estimate higher temperature values for the LGM than proxy records, thus an underestimation of LGM cooling by these datasets. Although not significant, this difference appears to be larger within mountains than outside mountains, meaning that LGM temperatures within mountain ranges are too warm compared to proxies. Thirdly, the bias in simulated LGM temperature estimates varies substantially across the globe. Paleoclimate datasets generally overestimate LGM cooling within mountains towards the Northern Hemisphere, compared to a relatively stable relationship towards the Southern Hemisphere, indicating a hemispheric bias in temperature estimations. Still, the direction of dataset-proxy disagreement often concurs amongst datasets, highlighting a consistent pattern in dataset behaviour despite regional differences. Fourthly, treeline reconstructions exhibit large elevational ranges within datasets and stark differences between datasets. Finally, coarser resolution datasets fail to capture smaller mountain ranges and islands in treeline reconstructions, underscoring the limitations of these datasets in representing finer geographical features.

Paleoclimate datasets vary vastly in spatial resolution. It is evident from our spatial comparison that not all datasets that cover the LGM have a suitable resolution for studies in mountain ranges (Fig. 3A). For example, coarser resolution datasets (Beyer, EcoClimate and PALEO-PGEM) fail to capture the gradual change of temperature with elevation, leading to counter-intuitive results (Fig. 3B). Limitations of paleoclimate models in mountains have been noted before, particularly their challenges in accurately simulating "regions with high gradients" (Brown et al. 2018), "regions with complex topography" (Lima-Ribeiro et al. 2015) or "topographic peculiarities" (Gamisch 2019). The more complex the topography, the more temperature information is lost with decreasing spatial resolution of the climate simulation. As mountain regions are of particular interest for the biogeographical community (Perrigo et al. 2020), it is important to consider the effect of the underlying climate simulation's spatial resolution on downscaled temperature estimations. Unfortunately, the varying temporal range and resolution of the datasets (see Table 1) could mean that the highest-resolution dataset available for the period of interest is insufficient to perform a sensible analysis.

Higher resolution, however, does not guarantee a more accurate representation of reality. For instance, downscaling methods allow researchers to computationally increase the spatial resolution, resulting in pseudo-replicated information (Taylor et al. 2012; Lima-Ribeiro et al. 2015). This is observed in Fig. 4, where CHELSA-TraCE21k showed the largest deviations from proxy estimates, despite having the highest spatial resolution. Additionally, the elevation-temperature relationship shown by the

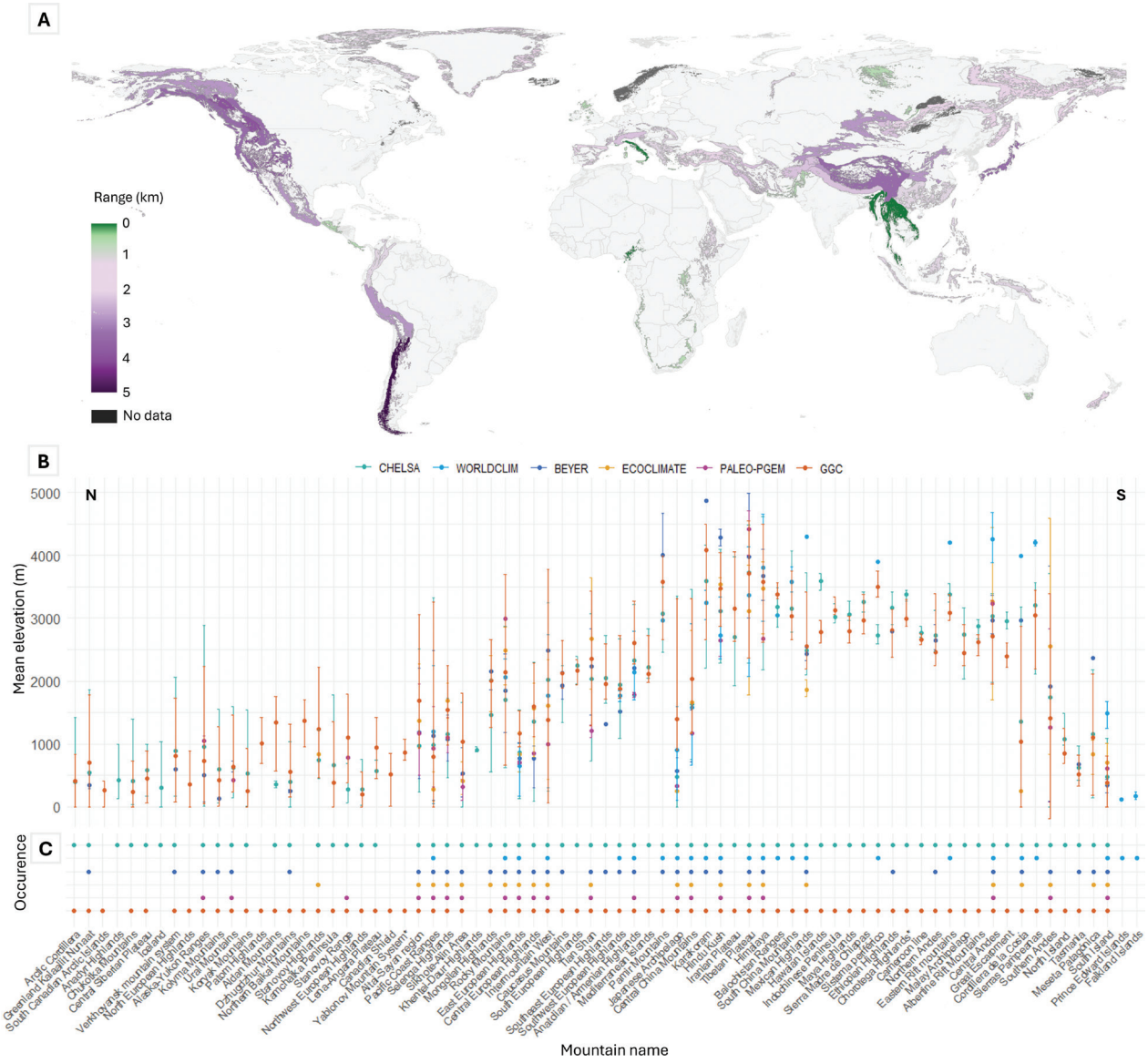

Figure 7. Reconstructed LGM treeline elevations and ranges derived from downscaled paleoclimate datasets. **A.** Maximum difference (i.e. range) of min/max treeline estimations for each dataset for different mountain ranges. Mountain ranges for which we had only one dataset were not calculated and are in black; **B.** Mean and range (min-max) of estimated LGM treeline elevations for each dataset and mountain range globally (GMBA level 3, Snethlage et al. (2022)). Dots represent mean estimated LGM treeline elevation and whiskers the min-max elevational range of estimated LGM treeline elevations; **C.** Occurrence of LGM treeline elevation estimates across datasets, indicating the presence (marked by a dot) or absence of treeline estimations for each mountain range. A dot indicates for which mountain range the dataset had values corresponding to the $T_{LGM} = T_{Treeline} \pm 0.25$ degrees. Mountains are ordered according to latitude from the north (left) to the south (right). Note that the mountains are plotted equidistant from one another and the latitude is, therefore, not uniformly spaced. GGC = global grid cooling.

CHELSA-TraCE21k dataset has a surprisingly sharp cut-off (Fig. 3B). The clustering of datapoints on the left side of the trend line in CHELSA-TraCE21k's scatterplot and the absence of data points on the right could reflect specific downscaling parameters such as thresholding, filtering or interpolation techniques. Such specificities are handled in all datasets and influence the distribution and range of temperature values across elevations (Varela et al. 2015). Furthermore, statistical downscaling (Box 1) relies on several assumptions that differ from reality, such as a stationary relationship between macro-and microclimates and a constant lapse rate over time, which can lead to inaccuracies in downscaled simulations (Salvi et al. 2016). This is also the case for CHELSA-TraCE21k, which is a statistical downscaling of the ERA-Interim reanalysis, with the temperature downscaling based on mean lapse rates and elevation (Karger et al. 2017). While these assumptions and techniques can improve spatial resolution, they also risk introducing biases that compromise the accuracy of temperature-elevation relationships, highlighting the need for caution when interpreting downscaled datasets.

We observe substantial spatial variability in LGM temperature estimates amongst different paleoclimate datasets, with a pronounced discrepancy between datasets and proxy records, especially in mountainous regions. These mismatches are not surprising, given the inherent difficulty of modelling and downscaling with a multitude of specific mechanisms and spatial variations at play (Harrison and Bartlein 2012). Overall, LGM cooling is underestimated by paleoclimate datasets (Fig. 4), which is in line with earlier findings of Kageyama et al. (2006), Masson-Delmotte et al. (2006), Bartlein et al. (2011) and Braconnot et al. (2012). Although not significant, this effect of underestimation is observed to be stronger within than outside mountain ranges for paleoclimate datasets. Such new insights are intuitive given that proxy records have indicated larger temperature changes at higher elevations (Harrison 2005; Loomis et al. 2017) and topographic-rich regions have been notoriously challenging to model (Lima-Ribeiro et al. 2015; Brown et al. 2018; Gamisch 2019). Furthermore, the dataset's temperature differences from proxy records are not randomly distributed in geographical space (Fig. 5). In South America, Central Europe and South Africa, LGM temperatures estimates from datasets are generally higher than proxy records (i.e. underestimation of cooling). In Alaska, Norway and Russia, LGM temperature estimates from datasets are generally colder than proxy records (i.e. overestimation of cooling). Varela et al. (2015) observed similar patterns for temperate regions when comparing GCM predictions for the LGM. Our study highlights that, also for downscaled paleoclimate datasets and especially for mountain regions, regional biases exist and should be considered when interpreting research outcomes, based on such datasets.

We also observe some outliers in the proxy data, located in the northernmost part of the Northern Hemisphere, with exceptionally large negative $\Delta T_{difference}$ values. These indicate that, for these locations, proxy records estimated higher LGM temperatures than the datasets, namely 8 and 13 °C. Many of these outliers occur at or near the former position of the Northern Hemisphere ice sheets, suggesting that a potential cause for these outliers is a modelled misspecification of the extent of these ice sheets, likely due to limited spatial resolution. This effect was possibly captured by the proxy records, but not by the simulations that underlie the datasets. Since these outlier records were present in every dataset we included, we believe it did not affect the observed inter-dataset variability.

Our results reveal that the global grid cooling method, despite its simplicity, has smaller incongruences within mountain ranges than outside in comparison to the proxy records (Figs 4, 6). A possible explanation for this is that the global grid cooling method applies a uniform temperature reduction across the globe without the introduction of dataset-specific biases, leading to more consistent and predictable results in regions with complex topography, such as mountain ranges. Still, it is surprising to see that this method has a closer similarity to the proxy-inferred LGM temperatures than CHELSA-TraCE21k's LGM temperature estimations. The difficulties in reconstructing temperature in mountains stem from the challenges of modelling complex topography, the scarcity of proxy data, variability in temperature lapse rates and microclimatic effects, amongst others (Gavin et al. 2014). It would be of interest to further investigate the potential of this method for mountain ranges, for example, by using regional temperature reconstructions derived from paleoenvironmental records (e.g. Chala et al. (2017); Rangel et al. (2018); Flantua et al. (2019)) — albeit as a heuristic approach until more robust paleoclimate datasets for mountains become available. Using regional temperature reconstructions has already shown great potential for spatial mapping of ecosystem shifts, for example, in island (Rijsdijk et al. 2014; Norder et al. 2018) and mountain biogeography (Flantua et al. 2019). Our results underscore that simplicity does not necessarily have to come at the expense of quality, offering many opportunities for environmental and biogeographical research depending on paleoclimatic reconstructions.

Regional differences in LGM cooling estimates, especially around the Tropics, are much less pronounced for the global grid cooling method compared to the paleoclimate datasets (Fig. 5). This might be related to the fact that there is often a lack of high-quality, long-term climatic and proxy data in tropical regions compared to temperate regions (Harrison 2005; Tovar et al. 2022). This scarcity of data can hinder the calibration and validation of simulations, making it more difficult to produce accurate LGM simulations. Additionally, tropical mountain regions, such as the Northern Andes, are characterised by complex climate dynamics with diverse vegetation, making it difficult to accurately capture these interactions (Tovar et al. 2022). In addition, temperature changes between the present and LGM were generally larger in temperate regions compared to the Tropics, due to the extensive ice sheets covering large parts of North America and Eurasia and polar amplification (Cao et al. 2019). Addressing these challenges by improving the calibration of paleoclimate simulations and incorporating more diverse proxy records from tropical mountains could significantly enhance our understanding of LGM climate dynamics in these complex regions.

There are substantial disagreements amongst paleoclimate datasets and across mountain ranges in treeline reconstructions, as shown by our results (Fig. 7B). The treeline reconstructions follow the well-known general pattern of lower treelines towards the poles and higher treelines around the Equator. Yet, the differences between datasets for a single mountain range are substantial (Fig. 7B). Depending on the dataset, the final reconstructed treeline can vary thousands of metres. Although some of the broad ranges between the minimum and maximum treeline reconstructions can be attributed to mountain ranges spanning over many latitudinal degrees (e.g. Southern Andes), others cannot (e.g. Selenga Highlands).

Underestimating LGM cooling places treelines too high, reducing the estimated alpine biome surface area, while overestimating LGM cooling places treelines too low, thus inflating the estimated alpine biome surface area. The magnitude of these over- and underestimations vary from

dataset to dataset and per region within a dataset. Considering how dataset choice influences the outcomes of the treeline reconstructions, such variations are equally expected to occur with any other boundary or biome reconstruction in mountain ranges. This has far-reaching implications for research concerning, amongst others, SDMs and ENMs, where species and biome range reconstructions are an important outcome to derive conclusions on, for example, refugia, climatic stability and velocity (e.g. Seo et al. (2008); Schorr et al. (2012); Gavin et al. (2014); Domic and Capriles (2021)). Inter-dataset variability (i.e. different datasets estimating different treeline elevations) and within-dataset divergence (i.e. broad estimated elevation range within a dataset) stresses the critical role of dataset choice on ecological reconstructions.

Modelling limitations are ubiquitous and perhaps even inevitable (Morrison and Lawrence 2023). The aim of this research is not to determine which dataset is better, but rather to highlight the magnitude and direction of intra- and inter-dataset variability and illustrate the implications for biogeographical research. It is difficult to determine whether the observed incongruences are caused by the underlying simulations of GCMs or RCMs, observations, statistical downscaling methods, or something else entirely. It is possible, for example, that the downscaling methods fail to capture elevation-dependent cooling in mountains ranges, which could explain the underestimated LGM cooling. Since the original simulations from ESMs, GCMs and RCMs are relatively coarse, the downscaled products could give false precision by trying to simulate elevational variations for high-resolution topographies that are absent in the original grids, leading to artefacts and biases in the downscaled data. It is also possible, however, that the biases were not introduced through downscaling, but already present in the original simulations and simply passed on to the downscaled dataset. Harrison et al. (2013), for example, found that paleoclimate models consistently underestimate land cooling and overestimate ocean surface cooling during the glacial period. Harrison et al. (2013) also found that models generally capture the direction of climate change, but struggled to reproduce spatial patterns, which is in line with the findings of this research. The datasets that were compared in this research, however, are based on various climate models and downscaling approaches (see Table 2), making it harder to pinpoint from where exactly the discrepancies come. Additional research is needed to investigate the underlying causes of the observed discrepancies.

Regarding paleoenvironmental proxy records, this study included proxies from a broad geographic distribution of records. Nonetheless, not all mountain ranges were represented by proxy records and, generally, only a single record was available per mountain range. While this limitation does not affect the observed differences between proxy records and datasets for a specific location, the addition of further records, especially for high elevations, could potentially refine the trends' strength and orientation currently observed. Furthermore, there are other potential proxy records (e.g. chironomids) and multi-proxy approaches that could improve the temperature simulations of paleoclimate models. When it comes to reconstructing past environments in mountains, regional paleoenvironmental proxy records can provide crucial information, but we should also consider the following: 1) despite global availability of such records, researchers cannot always rely on having sufficient records available in or near their study areas for the required time period. This is one of the reasons why downscaled paleoclimate datasets are so important and popular (Haywood et al. 2019); 2) proxy records also come with uncertainties and methodological limitations and cannot be treated as absolute truths (Harrison et al. 2016; Tierney et al. 2020a). For example, lower pCO_2 during the LGM could have had a negative effect on the water-use efficiency of plants and, thus, affect the climate-vegetation relationship (Street-Perrott et al. 1997). This could potentially make pollen assemblages appear colder (Cowling and Sykes 1999). However, while there seems to be an agreement on the impact of lower pCO_2 on pollen-based reconstructions of moisture availability (the reconstructions may be too dry relative to reality; Chevalier et al. (2020); Scheff et al. (2017)), there is no consensus about whether lower pCO_2 affects pollen-based reconstructions of temperature (Williams et al. 2000).

Combining a suite of proxy data with (multiple) paleoclimate simulations, a method called data assimilation, has been suggested as the best way to obtain LGM paleotemperature estimations for specific regions of interest (Schneider von Deimling et al. 2006; Worth et al. 2014). Paleoclimate data assimilation allows the refinement of model states, theoretically leading to more reliable climate reconstructions, as shown by, for example, Tierney et al. (2020a) and Osman et al. (2021). Although the integration of multiple simulations with proxy information helps reduce uncertainties in the climate estimates, this method remains dependent on the quality and spatial resolution of the underlying simulations. Furthermore, Williams et al. (2022) warn of circularity issues, where proxy networks, derived from certain biological proxies included in assimilation, can preclude the use of the resultant temperature estimates for studying, for example, ecoclimate sensitivity of the same proxies. Additionally, the inherent challenges of reconstructing climate at high resolution in topographically complex regions (i.e. mountains) or for regions or periods with sparse proxy records, also apply for data assimilation. Methods to tackle these issues are already in development, (see Tierney et al. (2020a) and Osman et al. (2021)), but still require further analysis.

We have highlighted the discrepancies for the LGM temperatures and illustrated the impacts for treeline reconstructions, but it is likely that the observed issues occur in other regions, moments in time and for other biome boundaries as well. Until paleoclimate datasets provide more reliable LGM temperature estimates for mountainous regions, the biogeographical community should remain cautious of these discrepancies. Researchers should consider these dataset limitations when interpreting climate reconstructions in mountain regions and use multiple datasets and methods to cross-validate their findings. We further suggest

avoiding datasets with strong variation or bias in regions of interest. Continued efforts to refine paleoclimate datasets and incorporate newly available proxy compilations from mountains and tropical regions will be essential for enhancing the reliability of these critical reconstructions. Such improvements are key to advancing our understanding of past biogeographical patterns and ecological dynamics that have shaped mountain ecosystems through time.

Conclusions

Downscaled paleoclimate datasets are extensively used in environmental and biogeographical research, with the Last Glacial Maximum (LGM) being a critical period due to its unique climatic conditions and significant impact on global ecosystems. However, the LGM temperature estimations from these datasets often differ from paleoenvironmental proxy records, with larger discrepancies observed within mountain ranges. A global grid cooling method, which lowers local temperatures by a global LGM estimate, provides closer-to-proxy estimations within mountains compared to downscaled paleoclimate datasets. Furthermore, coarse resolution datasets fail to capture the temperature gradient with elevation in mountainous regions.

We also highlight the disagreement within and amongst datasets and demonstrate that inter-dataset variability can substantially affect the outcomes of temperature-delimited boundary reconstructions of biomes. Not all paleoclimate datasets are suitable for studies on mountain ranges and significant incongruences and inconsistencies must be considered. Therefore, we call for greater awareness amongst the interdisciplinary community regarding the limitations of paleoclimate datasets, especially in mountainous areas. We advocate for more transparency and guidance in the methodologies of downscaled paleoclimate datasets for a broad audience and suggest that further research should focus on developing methods specifically tailored to capture the complex heterogeneity of mountain ranges, providing precise and reliable temperature estimations across time and space.

Acknowledgements

ESR, LS, ATW, JS, JAG and SGAF acknowledge financial support from Trond Mohn Research Foundation (TMF) and the University of Bergen for the start-up grant 'TMS-2022STG03' to S.G.A. Flantua. JS additionally acknowledges financial support from Research Foundation – Flanders (FWO) Odysseus Type II project GlaciersMD. OM is funded by the Czech Science Foundation PIF grant (GN23-06386I), by the Charles University Research Centre programme (UNCE/24/SCI/006) and by the Institutional Support for Science and Research of the Ministry of Education, Youth and Sports of the Czech Republic. We also thank two anonymous referees for their detailed feedback, which led to significant improvements of the publication.

Competing interest

The authors have declared that no competing interests exist.

Author contributions

ESR: Conceptualisation, methodology, software, validation, formal analysis, investigation, data curation, writing-original, visualisation. OM: Investigation, writing-review and editing. CP: Investigation, writing-review and editing. LS: Investigation, writing-review and editing. JS: Investigation, writing-review and editing. ATW: Methodology, software, data curation, writing-review and editing. JAG: Investigation, writing-review and editing, supervision. SGAF: Conceptualisation, methodology, resources, investigation, writing-review and editing, supervision, project administration, funding acquisition.

Data availability statement

Code and data required to perform the ΔT comparison, treeline reconstruction and all visualisations are available as a GitHub release on Zenodo: https://doi.org/10.5281/zenodo.14228272.

References

van Andel TH, Davies W (2003) Neanderthals and modern humans in the European landscape during the last glaciation: archaeological results of the Stage 3 Project. van Andel TH, Davies W (Eds). McDonald Institute for Archaeological Research, 265 pp. https://eprints.soton.ac.uk/41037/ [November 26, 2024]

Annan JD, Hargreaves JC (2015) A perspective on model-data surface temperature comparison at the Last Glacial Maximum. Quaternary Science Reviews 107: 1–10. https://doi.org/10.1016/j.quascirev.2014.09.019

Annan JD, Hargreaves JC, Mauritsen T (2022) A new global surface temperature reconstruction for the Last Glacial Maximum. Climate of the Past 18: 1883–1896. https://doi.org/10.5194/cp-18-1883-2022

Badgley C, Smiley TM, Cable R, Hoorn C, Perrigo A, Antonelli A (2018) Mountains, climate and mammals. John Wiley and Sons, Hoboken, NJ.

Baretto E, Holden P, Edwards N, Rangel TF (2022) PALEO-PGEM-Series: a spatial time series of the global climate over the last 5 million years (Plio-Pleistocene). https://doi.org/10.1111/geb.13683

Barreto E, Holden PB, Edwards NR, Rangel TF (2023) PALEO-PGEM-Series: A spatial time series of the global climate over the last 5 million years (Plio-Pleistocene). Global Ecology and Biogeography 32: 1034–1045. https://doi.org/10.1111/geb.13683

Bartlein PJ, Harrison SP, Brewer S, Connor S, Davis BAS, Gajewski K, Guiot J, Harrison-Prentice TI, Henderson A, Peyron O, Prentice IC, Scholze M, Seppä H, Shuman B, Sugita S, Thompson RS, Viau AE, Williams J, Wu H (2011) Pollen-based continental climate reconstructions at 6 and 21 ka: a global synthesis. Climate Dynamics 37: 775–802. https://doi.org/10.1007/s00382-010-0904-1

Beck HE, McVicar TR, Vergopolan N, Berg A, Lutsko NJ, Dufour A, Zeng Z, Jiang X, van Dijk AIJM, Miralles DG (2023) High-resolution (1 km) Köppen-Geiger maps for 1901–2099 based on constrained CMIP6 projections. Scientific Data 10: 724. https://doi.org/10.1038/s41597-023-02549-6

Beyer RM, Krapp M, Manica A (2020) High-resolution terrestrial climate, bioclimate and vegetation for the last 120,000 years. Scientific Data 7: 236. https://doi.org/10.1038/s41597-020-0552-1

Braconnot P, Harrison SP, Kageyama M, Bartlein PJ, Masson-Delmotte V, Abe-Ouchi A, Otto-Bliesner B, Zhao Y (2012) Evaluation of climate models using palaeoclimatic data. Nature Climate Change 2: 417–424. https://doi.org/10.1038/nclimate1456

Brown JL, Hill DJ, Dolan AM, Carnaval AC, Haywood AM (2018) PaleoClim, high spatial resolution paleoclimate surfaces for global land areas. Scientific Data 5: 180254. https://doi.org/10.1038/sdata.2018.254

Brown SC, Wigley TML, Otto-Bliesner BL, Fordham DA (2020) StableClim, continuous projections of climate stability from 21000 BP to 2100 CE at multiple spatial scales. Scientific Data 7: 335. https://doi.org/10.1038/s41597-020-00663-3

Cairns DM (2013) Alpine treelines: Functional ecology of the global high elevation tree limits. Arctic, Antarctic, and Alpine Research 45: 420–421. https://doi.org/10.1657/1938-4246-45.3.420

Cao J, Wang B, Liu J (2019) Attribution of the Last Glacial Maximum climate formation. Climate Dynamics 53: 1661–1679. https://doi.org/10.1007/s00382-019-04711-6

Carotenuto F, Di Febbraro M, Melchionna M, Castiglione S, Saggese F, Serio C, Mondanaro A, Passaro F, Loy A, Raia P (2016) The influence of climate on species distribution over time and space during the late Quaternary. Quaternary Science Reviews 149: 188–199. https://doi.org/10.1016/j.quascirev.2016.07.036

Chala D, Zimmermann NE, Brochmann C, Bakkestuen V (2017) Migration corridors for alpine plants among the 'sky islands' of eastern Africa: do they, or did they exist? Alpine Botany 127: 133–144. https://doi.org/10.1007/s00035-017-0184-z

Clark PU, Dyke AS, Shakun JD, Carlson AE, Clark J, Wohlfarth B, Mitrovica JX, Hostetler SW, McCabe AM (2009) The Last Glacial Maximum. Science 325: 710–714. https://doi.org/10.1126/science.1172873

Chevalier M, Davis BA, Heiri O, Seppä H, Chase BM, Gajewski K, Lacourse T, Telford RJ, Finsinger W, Guiot J, Kühl N, Maezumi SY, Tipton JR, Carter VA, Brussel T, Phelps LN, Dawson A, Zanon M, Vallé F, Nolan C, Mauri A, de Vernal A, Izumi K, Holmström L, Marsicek J, Goring S, Sommer PS, Chaput M, Kupriyanov D (2020) Pollen-based climate reconstruction techniques for late Quaternary studies. Earth-Science Reviews 210: 103384. https://doi.org/10.1016/j.earscirev.2020.103384

Collevatti RG, Terribile LC, de Oliveira G, Lima-Ribeiro MS, Nabout JC, Rangel TF, Diniz-Filho JAF (2013) Drawbacks to palaeodistribution modelling: the case of South American seasonally dry forests. Journal of Biogeography 40: 345–358. https://doi.org/10.1111/jbi.12005

Copernicus (2021) What is Statistical and Dynamical downscaling? https://climate.copernicus.eu/sites/default/files/2021-01/infosheet8.pdf [January 8, 2025]

Cowling SA, Sykes MT (1999) Physiological Significance of Low Atmospheric CO_2 for Plant–Climate Interactions. Quaternary Research 52: 237–242. https://doi.org/10.1006/qres.1999.2065

Daniels LD, Veblen TT (2004) Spatiotemporal Influences of Climate on Altitudinal Treeline in Northern Patagonia. Ecology 85: 1284–1296. https://doi.org/10.1890/03-0092

Danielson JJ, Gesch DB (2011) Global multi-resolution terrain elevation data 2010 (GMTED2010). U.S. Geological Survey. Open-File Report. https://doi.org/10.3133/ofr20111073

Domic AI, Capriles JM (2021) Distribution shifts in habitat suitability and hotspot refugia of Andean tree species from the last glacial maximum to the Anthropocene. Neotropical Biodiversity 7: 297–309. https://doi.org/10.1080/23766808.2021.1957652

Dunne JP, John JG, Adcroft AJ, Griffies SM, Hallberg RW, Shevliakova E, Stouffer RJ, Cooke W, Dunne KA, Harrison MJ, Krasting JP, Malyshev SL, Milly PCD, Phillipps PJ, Sentman LT, Samuels BL, Spelman MJ, Winton M, Wittenberg AT, Zadeh N (2012) GFDL's ESM2 Global Coupled Climate–Carbon Earth System Models. Part I: Physical Formulation and Baseline Simulation Characteristics. Journal of Climate 25: 6646–6665. https://doi.org/10.1175/JCLI-D-11-00560.1

Dunne JP, John JG, Shevliakova E, Stouffer RJ, Krasting JP, Malyshev SL, Milly PCD, Sentman LT, Adcroft AJ, Cooke W, Dunne KA, Griffies SM, Hallberg RW, Harrison MJ, Levy H, Wittenberg AT, Phillips PJ, Zadeh N (2013) GFDL's ESM2 Global Coupled Climate–Carbon Earth System Models. Part II: Carbon System Formulation and Baseline Simulation Characteristics*. https://doi.org/10.1175/JCLI-D-12-00150.1

Erb MP, McKay NP, Steiger N, Dee S, Hancock C, Ivanovic RF, Gregoire LJ, Valdes P (2022) Reconstructing Holocene temperatures in time and space using paleoclimate data assimilation. Climate of the Past 18: 2599–2629. https://doi.org/10.5194/cp-18-2599-2022

Esri HERE, Garmin FAO, NOAA, USGS (2015) Light Gray Canvas. https://www.arcgis.com/home/item.html?id=979c6cc89af9449cbeb5342a439c6a76 [December 1, 2023]

Farrera I, Harrison SP, Prentice IC, Ramstein G, Guiot J, Bartlein PJ, Bonnefille R, Bush M, Cramer W, von Grafenstein U, Holmgren K, Hooghiemstra H, Hope G, Jolly D, Lauritzen S-E, Ono Y, Pinot S, Stute M, Yu G (1999) Tropical climates at the Last Glacial Maximum: a new synthesis of terrestrial palaeoclimate data. I. Vegetation, lake-levels and geochemistry. Climate Dynamics 15: 823–856. https://doi.org/10.1007/s003820050317

Fick SE, Hijmans RJ (2017) WorldClim 2: new 1-km spatial resolution climate surfaces for global land areas. International Journal of Climatology 37: 4302–4315. https://doi.org/10.1002/joc.5086

Flantua SGA, O'Dea A, Onstein RE, Giraldo C, Hooghiemstra H (2019) The flickering connectivity system of the north Andean páramos. Journal of Biogeography 46: 1808–1825. https://doi.org/10.1111/jbi.13607

Gamisch A (2019) Oscillayers: A dataset for the study of climatic oscillations over Plio-Pleistocene time-scales at high spatial-temporal resolution. Global Ecology and Biogeography 28: 1552–1560. https://doi.org/10.1111/geb.12979

Garzón MB, Sánchez de Dios R, Sainz Ollero H (2008) The evolution of the *Pinus sylvestris* L. area in the Iberian Peninsula from the last glacial maximum to 2100 under climate change. The Holocene 18: 705–714. https://doi.org/10.1177/0959683608091781

Gates WL (1976) The Numerical Simulation of Ice-Age Climate with a Global General Circulation Model. https://journals.ametsoc.org/view/journals/atsc/33/10/1520-0469_1976_033_1844_tnsoia_2_0_co_2.xml [November 26, 2024]

Gavin DG, Fitzpatrick MC, Gugger PF, Heath KD, Rodríguez-Sánchez F, Dobrowski SZ, Hampe A, Hu FS, Ashcroft MB, Bartlein PJ, Blois JL, Carstens BC, Davis EB, de Lafontaine G, Edwards ME, Fernandez M, Henne PD, Herring EM, Holden ZA, Kong W, Liu J, Magri D, Matzke NJ, McGlone MS, Saltré F, Stigall AL, Tsai Y-HE, Williams JW (2014) Climate refugia: joint inference from fossil records, species distribution models and phylogeography. New Phytologist 204: 37–54. https://doi.org/10.1111/nph.12929

Greenwood S, Jump AS (2014) Consequences of treeline shifts for the diversity and function of high altitude ecosystems. Arctic, Antarctic, and Alpine Research 46: 829–840. https://doi.org/10.1657/1938-4246-46.4.829

Hansen J, Sato M, Russell G, Kharecha P (2013) Climate sensitivity, sea level and atmospheric carbon dioxide. Philosophical Transactions of the Royal Society A: Mathematical, Physical and Engineering Sciences 371: 20120294. https://doi.org/10.1098/rsta.2012.0294

Harrison S, Noss R (2017) Endemism hotspots are linked to stable climatic refugia. Annals of Botany 119: 207–214. https://doi.org/10.1093/aob/mcw248

Harrison SP (2005) Snowlines at the last glacial maximum and tropical cooling. Quaternary International 138–139: 5–7. https://doi.org/10.1016/j.quaint.2005.02.002

Harrison SP, Bartlein P (2012) Chapter 14 - Records from the Past, Lessons for the Future: What the Palaeorecord Implies about Mechanisms of Global Change. In: Henderson-Sellers A, McGuffie K (Eds) The Future of the World's Climate (Second Edition). Elsevier, Boston, 403–436. https://doi.org/10.1016/B978-0-12-386917-3.00014-2

Harrison SP, Bartlein PJ, Brewer S, Prentice IC, Boyd M, Hessler I, Holmgren K, Izumi K, Willis K (2013) Climate model benchmarking with glacial and mid-Holocene climates. Climate Dynamics 43: 671–688. https://doi.org/10.1007/s00382-013-1922-6

Harrison SP, Bartlein PJ, Prentice IC (2016) What have we learnt from palaeoclimate simulations? Journal of Quaternary Science 31: 363–385. https://doi.org/10.1002/jqs.2842

Haywood AM, Valdes PJ, Markwick PJ (2004) Cretaceous (Wealden) climates: a modelling perspective. Cretaceous Research 25: 303–311. https://doi.org/10.1016/j.cretres.2004.01.005

Haywood AM, Valdes PJ, Aze T, Barlow N, Burke A, Dolan AM, von der Heydt AS, Hill DJ, Jamieson SSR, Otto-Bliesner BL, Salzmann U, Saupe E, Voss J (2019) What can Palaeoclimate Modelling do for you? Earth Systems and Environment 3: 1–18. https://doi.org/10.1007/s41748-019-00093-1

Hijmans RJ, Cameron SE, Parra JL, Jones PG, Jarvis A (2005) Very high resolution interpolated climate surfaces for global land areas. International Journal of Climatology 25: 1965–1978. https://doi.org/10.1002/joc.1276

Hik DS, Williamson SN (2019) Need for mountain weather stations climbs. Science 366: 1083–1083. https://doi.org/10.1126/science.aaz7450

Hostetler S (2015) Climate models: applications to understand past climates and climate change. USGS - Earth Science Matters Newsletter. https://www.usgs.gov/news/climate-models-applications-understand-past-climates-and-climate-change [July 17, 2024]

Hughes PD, Gibbard PL, Ehlers J (2013) Timing of glaciation during the last glacial cycle: evaluating the concept of a global 'Last Glacial Maximum' (LGM). Earth-Science Reviews 125: 171–198. https://doi.org/10.1016/j.earscirev.2013.07.003

Jansen E, Overpeck J, Briffa KR, Duplessy J-C, Joos F, Masson-Delmotte V, Olago D, Otto-Bliesner B, Peltier WR, Rahmstorf S, Ramesh R, Raynaud D, Rind D, Solomina O, Villalba R, Zhang D, Barnola J-M, Bauer E, Brady E, Chandler M, Cole J, Cook E, Cortijo E, Dokken T, Fleitmann D, Kageyama M, Khodri M, Labeyrie L, Laine A, Levermann A, Lie Ø, Loutre M-F, Matsumoto K, Monnin E, Mosley-Thompson E, Muhs D, Muscheler R, Osborn T, Paasche Ø, Parrenin F, Plattner G-K, Pollack H, Spahni R, Stott LD, Thompson L, Waelbroeck C, Wiles G, Zachos J, Zhengteng G, Jouzel J, Mitchell J, Solomon S, Qin D, Manning M, Chen Z, Marquis M, Averyt KB, Tignor M, Miller HL (2007) Palaeoclimate. In: Solomon S, Qin D, Manning M, Chen Z, Marquis M, Averyt KB, Tignor M, Miller HL (Eds) Contribution of Working Group I to the Fourth Assessment Report of the Intergovernmental Panel on Climate Change. Cambridge University Press. https://hal.science/hal-03375712

Jobbágy EG, Jackson RB (2000) Global controls of forest line elevation in the northern and southern hemispheres. Global Ecology and Biogeography 9: 253–268. https://doi.org/10.1046/j.1365-2699.2000.00162.x

Jouzel J, Masson-Delmotte V (2007) EPICA Dome C Ice Core 800KYr deuterium data and temperature estimates. Supplement to: Jouzel, Jean; Masson-Delmotte, Valerie; Cattani, Olivier; Dreyfus, Gabrielle; Falourd, Sonia; Hoffmann, G; Minster, Bénédicte; Nouet, Julius; Barnola, Jean-Marc; Chappellaz, Jérôme A; Fischer, Hubertus; Gallet, J C; Johnsen, Sigfús Jóhann; Leuenberger, Markus Christian; Loulergue, Laetitia; Luethi, D; Oerter, Hans; Parrenin, Frédéric; Raisbeck, Grant M; Raynaud, Dominique; Schilt, Adrian; Schwander, Jakob; Selmo, Enricomaria; Souchez, Roland A; Spahni, Renato; Stauffer, Bernhard; Steffensen, Jørgen Peder; Stenni, Barbara; Stocker, Thomas F; Tison, Jean-Louis; Werner, Martin; Wolff, Eric William (2007): Orbital and millennial Antarctic climate variability over the past 800,000 years. Science 317(5839): 793–797. https://doi.org/10.1126/science.1141038

Jouzel J, Masson-Delmotte V, Cattani O, Dreyfus G, Falourd S, Hoffmann G, Minster B, Nouet J, Barnola JM, Chappellaz J, Fischer H, Gallet JC, Johnsen S, Leuenberger M, Loulergue L, Luethi D, Oerter H, Parrenin F, Raisbeck G, Raynaud D, Schilt A, Schwander J, Selmo E, Souchez R, Spahni R, Stauffer B, Steffensen JP, Stenni B, Stocker TF, Tison JL, Werner M, Wolff EW (2007) Orbital and Millennial Antarctic Climate Variability over the Past 800,000 Years. Science 317: 793–796. https://doi.org/10.1126/science.1141038

Kageyama M, Paillard D (2021) Modeling and paleoclimatology. In: Ramstein G, Landais A, Bouttes N, Sepulchre P, Govin A (Eds) Paleoclimatology. Springer International Publishing, Cham, 319–342. https://doi.org/10.1007/978-3-030-24982-3_25

Kageyama M, Laîné A, Abe-Ouchi A, Braconnot P, Cortijo E, Crucifix M, de Vernal A, Guiot J, Hewitt CD, Kitoh A, Kucera M, Marti O, Ohgaito R, Otto-Bliesner B, Peltier WR, Rosell-Melé A, Vettoretti G, Weber SL, Yu Y (2006) Last Glacial Maximum temperatures over the North Atlantic, Europe and western Siberia: a comparison between PMIP models, MARGO sea–surface temperatures and pollen-based reconstructions. Quaternary Science Reviews 25: 2082–2102. https://doi.org/10.1016/j.quascirev.2006.02.010

Kandziora M, Gorospe JM, Salomon L, Vásquez DLA, Vargas MP, Kolář F, Sklenář P, Schmickl R (2024) The ghost of past climate acting on present-day plant diversity: Lessons from a climate-based delimitation of the tropical alpine ecosystem. Journal of Systematics and Evolution 62: 275–290. https://doi.org/10.1111/jse.13048

Karger DN, Conrad O, Böhner J, Kawohl T, Kreft H, Soria-Auza RW, Zimmermann NE, Linder HP, Kessler M (2017) Climatologies at high resolution for the earth's land surface areas. Scientific Data 4: 170122. https://doi.org/10.1038/sdata.2017.122

Karger DN, Nobis MP, Normand S, Graham CH, Zimmermann NE (2023) CHELSA-TraCE21k – high-resolution (1km) downscaled transient temperature and precipitation data since the Last Glacial Maximum. Climate of the Past 19: 439–456. https://doi.org/10.5194/cp-19-439-2023

Kienle DR, Irl SDH, Beierkuhnlein C (2023) Mass elevation effect and continentality have a stronger impact on global treelines than spatial isolation. Global Ecology and Biogeography 32: 1087–1097. https://doi.org/10.1111/geb.13689

Kohfeld KE, Harrison SP (2000) How well can we simulate past climates? Evaluating the models using global palaeoenvironmental datasets. Quaternary Science Reviews 19: 321–346. https://doi.org/10.1016/S0277-3791(99)00068-2

Körner C (2007) Climatic Treelines: Conventions, Global Patterns, Causes (Klimatische Baumgrenzen: Konventionen, globale Muster, Ursachen). Erdkunde 61: 316–324. https://doi.org/10.3112/erdkunde.2007.04.02

Körner C (2021) Alpine treelines. In: Körner C (Ed.) Alpine Plant Life: Functional Plant Ecology of High Mountain Ecosystems. Springer International Publishing, Cham, 141–173. https://doi.org/10.1007/978-3-030-59538-8_7

Körner C, Paulsen J (2004) A world-wide study of high altitude treeline temperatures. Journal of Biogeography 31: 713–732. https://doi.org/10.1111/j.1365-2699.2003.01043.x

Körner C, Hoch G (2023) Not every high-latitude or high-elevation forest edge is a treeline. Journal of Biogeography 50: 838–845. https://doi.org/10.1111/jbi.14593

Krapp M, Beyer RM, Edmundson SL, Valdes PJ, Manica A (2021) A statistics-based reconstruction of high-resolution global terrestrial climate for the last 800,000 years. Scientific Data 8: 228. https://doi.org/10.1038/s41597-021-01009-3

Lima-Ribeiro MS, Varela S, González-Hernández J, Oliveira G de, Diniz-Filho JAF, Terribile LC (2015) EcoClimate: a database of climate data from multiple models for past, present, and future for macroecologists and biogeographers. Biodiversity Informatics 10. https://doi.org/10.17161/bi.v10i0.4955

Loomis SE, Russell JM, Verschuren D, Morrill C, De Cort G, Sinninghe Damsté JS, Olago D, Eggermont H, Street-Perrott FA, Kelly MA (2017) The tropical lapse rate steepened during the Last Glacial Maximum. Science Advances 3: e1600815. https://doi.org/10.1126/sciadv.1600815

Ludwig P, Gómez-Navarro JJ, Pinto JG, Raible CC, Wagner S, Zorita E (2019) Perspectives of regional paleoclimate modeling. Annals of the New York Academy of Sciences 1436: 54–69. https://doi.org/10.1111/nyas.13865

Mark BG, Harrison SP, Spessa A, New M, Evans DJA, Helmens KF (2005) Tropical snowline changes at the last glacial maximum: A global assessment. Quaternary International 138–139: 168–201. https://doi.org/10.1016/j.quaint.2005.02.012

Martínez-Meyer E, Peterson AT (2006) Conservatism of ecological niche characteristics in North American plant species over the Pleistocene-to-Recent transition. Journal of Biogeography 33: 1779–1789. https://doi.org/10.1111/j.1365-2699.2006.01482_33_10.x

Masson-Delmotte V, Kageyama M, Braconnot P, Charbit S, Krinner G, Ritz C, Guilyardi E, Jouzel J, Abe-Ouchi A, Crucifix M, Gladstone RM, Hewitt CD, Kitoh A, LeGrande AN, Marti O, Merkel U, Motoi T, Ohgaito R, Otto-Bliesner B, Peltier WR, Ross I, Valdes PJ, Vettoretti G, Weber SL, Wolk F, Yu Y (2005) Past and future polar amplification of climate change: climate model intercomparisons and ice-core constraints. Climate Dynamics 26: 513–529. https://doi.org/10.1007/s00382-005-0081-9

Masson-Delmotte V, Dreyfus G, Braconnot P, Johnsen S, Jouzel J, Kageyama M, Landais A, Loutre M-F, Nouet J, Parrenin F, Raynaud D, Stenni B, Tuenter E (2006) Past temperature reconstructions from deep ice cores: relevance for future climate change. Climate of the Past 2: 145–165. https://doi.org/10.5194/cp-2-145-2006

Mix AC, Bard E, Schneider R (2001) Environmental processes of the ice age: land, oceans, glaciers (EPILOG). Quaternary Science Reviews 20: 627–657. https://doi.org/10.1016/S0277-3791(00)00145-1

Morrison MA, Lawrence P (2023) Understanding Model-Based Uncertainty in Climate Science. In: Handbook of philosophy of climate change. Springer International Publishing, 1–21. https://doi.org/10.1007/978-3-030-16960-2_154-1

Muellner-Riehl AN, Schnitzler J, Kissling WD, Mosbrugger V, Rijsdijk KF, Seijmonsbergen AC, Versteegh H, Favre A (2019) Origins of global mountain plant biodiversity: Testing the 'mountain-geobiodiversity hypothesis.' Journal of Biogeography 46: 2826–2838. https://doi.org/10.1111/jbi.13715

Nogués-Bravo D (2009) Predicting the past distribution of species climatic niches. Global Ecology and Biogeography 18: 521–531. https://doi.org/10.1111/j.1466-8238.2009.00476.x

Nolan C, Overpeck JT, Allen JRM, Anderson PM, Betancourt JL, Binney HA, Brewer S, Bush MB, Chase BM, Cheddadi R, Djamali M, Dodson J, Edwards ME, Gosling WD, Haberle S, Hotchkiss SC, Huntley B, Ivory SJ, Kershaw AP, Kim S-H, Latorre C, Leydet M, Lézine A-M, Liu K-B, Liu Y, Lozhkin AV, McGlone MS, Marchant RA, Momohara A, Moreno PI, Müller S, Otto-Bliesner BL, Shen C, Stevenson J, Takahara H, Tarasov PE, Tipton J, Vincens A, Weng C, Xu Q, Zheng Z, Jackson ST (2018) Past and future global transformation of terrestrial ecosystems under climate change. Science 361: 920–923. https://doi.org/10.1126/science.aan5360

Norder SJ, Baumgartner JB, Borges PAV, Hengl T, Kissling WD, van Loon EE, Rijsdijk KF (2018) A global spatially explicit database of changes in island palaeo-area and archipelago configuration during the late Quaternary. Global Ecology and Biogeography 27: 500–505. https://doi.org/10.1111/geb.12715

Osman MB, Tierney JE, Zhu J, Tardif R, Hakim GJ, King J, Poulsen CJ (2021) Globally resolved surface temperatures since the Last Glacial Maximum. Nature 599: 239–244. https://doi.org/10.1038/s41586-021-03984-4

Paulsen J, Körner C (2014) A climate-based model to predict potential treeline position around the globe. Alpine Botany 124: 1–12. https://doi.org/10.1007/s00035-014-0124-0

Pedersen EJ, Miller DL, Simpson GL, Ross N (2019) Hierarchical generalized additive models in ecology: an introduction with mgcv. PeerJ 7: e6876. https://doi.org/10.7717/peerj.6876

Pepin NC, Arnone E, Gobiet A, Haslinger K, Kotlarski S, Notarnicola C, Palazzi E, Seibert P, Serafin S, Schöner W, Terzago S, Thornton JM, Vuille M, Adler C (2022) Climate changes and their elevational patterns in the mountains of the world. Reviews of Geophysics 60: e2020RG000730. https://doi.org/10.1029/2020RG000730

Perrigo A, Hoorn C, Antonelli A (2020) Why mountains matter for biodiversity. Journal of Biogeography 47: 315–325. https://doi.org/10.1111/jbi.13731

Rangel TF, Edwards NR, Holden PB, Diniz-Filho JAF, Gosling WD, Coelho MTP, Cassemiro FAS, Rahbek C, Colwell RK (2018) Modeling the ecology and evolution of biodiversity: Biogeographical cradles, museums, and graves. Science 361: eaar5452. https://doi.org/10.1126/science.aar5452

Rijsdijk KF, Hengl T, Norder SJ, Otto R, Emerson BC, Ávila SP, López H, van Loon EE, Tjørve E, Fernández-Palacios JM (2014) Quantifying surface-area changes of volcanic islands driven by Pleistocene sea-level cycles: biogeographical implications for the Macaronesian archipelagos. Journal of Biogeography 41: 1242–1254. https://doi.org/10.1111/jbi.12336

Salvi K, Ghosh S, Ganguly AR (2016) Credibility of statistical downscaling under nonstationary climate. Climate Dynamics 46: 1991–2023. https://doi.org/10.1007/s00382-015-2688-9

Sandel B, Arge L, Dalsgaard B, Davies RG, Gaston KJ, Sutherland WJ, Svenning J-C (2011) The influence of Late Quaternary Climate-Change velocity on species endemism. Science 334: 660–664. https://doi.org/10.1126/science.1210173

Scheff J, Seager R, Liu H, Coats S (2017) Are glacials dry? Consequences for paleoclimatology and for greenhouse warming. Journal of Climate 30(17): 6593–6609. https://doi.org/10.1175/JCLI-D-16-0854.1

Schneider von Deimling T, Ganopolski A, Held H, Rahmstorf S (2006) How cold was the Last Glacial Maximum? Geophysical Research Letters 33: L14709. https://doi.org/10.1029/2006GL026484

Schorr G, Holstein N, Pearman PB, Guisan A, Kadereit JW (2012) Integrating species distribution models (SDMs) and phylogeography for two species of Alpine *Primula*. Ecology and Evolution 2: 1260–1277. https://doi.org/10.1002/ece3.100

Seo C, Thorne JH, Hannah L, Thuiller W (2008) Scale effects in species distribution models: implications for conservation planning under climate change. Biology Letters 5: 39–43. https://doi.org/10.1098/rsbl.2008.0476

Shafer SL, Bartlein PJ, Whitlock C (2005) Understanding the spatial heterogeneity of global environmental change in mountain regions. In: Huber UM, Bugmann HKM, Reasoner MA (Eds) Global change and mountain regions: An overview of current knowledge. Springer Netherlands, Dordrecht, 21–30. https://doi.org/10.1007/1-4020-3508-X_3

Shi X, Werner M, Yang H, D'Agostino R, Liu J, Yang C, Lohmann G (2023) Unraveling the complexities of the Last Glacial Maximum climate: the role of individual boundary conditions and forcings. Climate of the Past 19: 2157–2175. https://doi.org/10.5194/cp-19-2157-2023

Snethlage MA, Geschke J, Spehn EM, Ranipeta A, Yocco NG, Körner C, Jetz W, Fischer M, Urbach D (2021) GMBA Mountain Inventory v2. https://doi.org/10.48601/EARTHENV-T9K2-1407

Snethlage MA, Geschke J, Ranipeta A, Jetz W, Yoccoz NG, Körner C, Spehn EM, Fischer M, Urbach D (2022) A hierarchical inventory of the world's mountains for global comparative mountain science. Scientific Data 9: 149. https://doi.org/10.1038/s41597-022-01256-y

Stigall AL (2013) Analysing links between biogeography, niche stability and speciation: the impact of complex feedbacks on macroevolutionary patterns. Palaeontology 56: 1225–1238. https://doi.org/10.1111/pala.12003

Street-Perrott FA, Huang Y, Perrott RA, Eglinton G, Barker P, Khelifa LB, Harkness DD, Olago DO (1997) Impact of lower atmospheric carbon dioxide on tropical mountain ecosystems. Science 278: 1422–1426. https://doi.org/10.1126/science.278.5342.1422

Svenning J-C, Fløjgaard C, Marske KA, Nógues-Bravo D, Normand S (2011) Applications of species distribution modeling to paleobiology. Quaternary Science Reviews 30: 2930–2947. https://doi.org/10.1016/j.quascirev.2011.06.012

Tang CQ, Matsui T, Ohashi H, Dong Y-F, Momohara A, Herrando-Moraira S, Qian S, Yang Y, Ohsawa M, Luu HT, Grote PJ, Krestov PV, LePage B, Werger M, Robertson K, Hobohm C, Wang C-Y, Peng M-C, Chen X, Wang H-C, Su W-H, Zhou R, Li S, He L-Y, Yan K, Zhu M-Y, Hu J, Yang R-H, Li W-J, Tomita M, Wu Z-L, Yan H-Z, Zhang G-F, He H, Yi S-R, Gong H, Song K, Song D, Li X-S, Zhang Z-Y, Han P-B, Shen L-Q, Huang D-S, Luo K, López-Pujol J (2018) Identifying long-term stable refugia for relict plant species in East Asia. Nature Communications 9: 4488. https://doi.org/10.1038/s41467-018-06837-3

Taylor KE, Stouffer RJ, Meehl GA (2012) An overview of CMIP5 and the experiment design. Bulletin of the American Meteorological Society 93: 485–498. https://doi.org/10.1175/BAMS-D-11-00094.1

Testolin R, Attorre F, Jiménez-Alfaro B (2020) Global distribution and bioclimatic characterization of alpine biomes. Ecography 43: 779–788. https://doi.org/10.1111/ecog.05012

Thornton JM, Pepin N, Shahgedanova M, Adler C (2022) Coverage of *in situ* climatological observations in the world's mountains. Frontiers in Climate 4: 814181. https://doi.org/10.3389/fclim.2022.814181

Tierney JE, Zhu J, King J, Malevich SB, Hakim GJ, Poulsen CJ (2020a) Glacial cooling and climate sensitivity revisited. Nature 584: 569–573. https://doi.org/10.1038/s41586-020-2617-x

Tierney JE, Poulsen CJ, Montañez IP, Bhattacharya T, Feng R, Ford HL, Hönisch B, Inglis GN, Petersen SV, Sagoo N, Tabor CR, Thirumalai K, Zhu J, Burls NJ, Foster GL, Goddéris Y, Huber BT, Ivany LC, Kirtland Turner S, Lunt DJ, McElwain JC, Mills BJW, Otto-Bliesner BL, Ridgwell A, Zhang YG (2020b) Past climates inform our future. Science 370: eaay3701. https://doi.org/10.1126/science.aay3701

Tovar C, Carril AF, Gutiérrez AG, Ahrends A, Fita L, Zaninelli P, Flombaum P, Abarzúa AM, Alarcón D, Aschero V, Báez S, Barros A, Carilla J, Ferrero ME, Flantua SGA, Gonzáles P, Menéndez CG, Pérez-Escobar OA, Pauchard A, Ruscica RC, Särkinen T, Sörensson AA, Srur A, Villalba R, Hollingsworth PM (2022) Understanding climate change impacts on biome and plant distributions in the Andes: Challenges and opportunities. Journal of Biogeography 49: 1420–1442. https://doi.org/10.1111/jbi.14389

Varela S, Lobo JM, Hortal J (2011) Using species distribution models in paleobiogeography: A matter of data, predictors and concepts. Palaeogeography, Palaeoclimatology, Palaeoecology 310: 451–463. https://doi.org/10.1016/j.palaeo.2011.07.021

Varela S, Lima-Ribeiro MS, Terribile LC (2015) A Short Guide to the Climatic Variables of the Last Glacial Maximum for Biogeographers. Rebelo H (Ed.). PLOS ONE 10: e0129037. https://doi.org/10.1371/journal.pone.0129037

Waelbroeck C, Paul A, Kucera M, Rosell-Melé A, Weinelt M, Schneider R, Mix AC, Abelmann A, Armand L, Bard E, Barker S, Barrows TT, Benway H, Cacho I, Chen M-T, Cortijo E, Crosta X, de Vernal A, Dokken T, Duprat J, Elderfield H, Eynaud F, Gersonde R, Hayes A, Henry M, Hillaire-Marcel C, Huang C-C, Jansen E, Juggins S, Kallel N, Kiefer T, Kienast M, Labeyrie L, Leclaire H, Londeix L,

Mangin S, Matthiessen J, Marret F, Meland M, Morey AE, Mulitza S, Pflaumann U, Pisias NG, Radi T, Rochon A, Rohling EJ, Sbaffi L, Schäfer-Neth C, Solignac S, Spero H, Tachikawa K, Turon J-L, MARGO Project Members (2009) Constraints on the magnitude and patterns of ocean cooling at the Last Glacial Maximum. Nature Geoscience 2: 127–132. https://doi.org/10.1038/ngeo411

Werneck FP, Costa GC, Colli GR, Prado DE, Sites Jr JW (2011) Revisiting the historical distribution of Seasonally Dry Tropical Forests: new insights based on palaeodistribution modelling and palynological evidence. Global Ecology and Biogeography 20: 272–288. https://doi.org/10.1111/j.1466-8238.2010.00596.x

Williams JW, Iii TW, Shurman BN, Bartlein PJ (2000) Do low CO_2 concentrations affect pollen-based reconstructions of LGM climates? A response to "Physiological significance of low atmospheric CO_2 for plant–climate interactions" by Cowling and Sykes. Quaternary Research 53: 402–404. https://doi.org/10.1006/qres.2000.2131

Williams JW, Huntley B, Seddon AWR (2022) Climate sensitivity and ecoclimate sensitivity: Theory, usage, and past implications for future biospheric responses. Current Climate Change Reports 8: 1–16. https://doi.org/10.1007/s40641-022-00179-5

Worth JRP, Williamson GJ, Sakaguchi S, Nevill PG, Jordan GJ (2014) Environmental niche modelling fails to predict Last Glacial Maximum refugia: niche shifts, microrefugia or incorrect palaeoclimate estimates? Global Ecology and Biogeography 23: 1186–1197. https://doi.org/10.1111/geb.12239

Zhu J, Poulsen CJ (2021) Last Glacial Maximum (LGM) climate forcing and ocean dynamical feedback and their implications for estimating climate sensitivity. Climate of the Past 17: 253–267. https://doi.org/10.5194/cp-17-253-2021

Supplementary materials

Supplementary material 1

Supplementary tables S1, S2 (.docx)
Link: https://doi.org/10.21425/fob.18.135871.suppl1